Bioorganic & Medicinal Chemistry xxx (xxxx) xxx–xxx

Contents lists available at ScienceDirect

Bioorganic & Medicinal Chemistry

journal homepage: www.elsevier.com/locate/bmc

Alkynamide phthalazinones as a new class of TbrPDEB1 inhibitors

Erik de Heuvel[a], Abhimanyu K. Singh[b], Ewald Edink[a], Tiffany van der Meer[a], Melanie van der Woude[a], Payman Sadek[a], Mikkel P. Krell-Jørgensen[a], Toine van den Bergh[c], Johan Veerman[c], Guy Caljon[d], Titilola D. Kalejaiye[e], Maikel Wijtmans[a], Louis Maes[d], Harry P. de Koning[e], Geert Jan Sterk[a], Marco Siderius[a], Iwan J.P. de Esch[a], David G. Brown[b], Rob Leurs[a,*]

[a] Division of Medicinal Chemistry, Amsterdam Institute for Molecules, Medicines and Systems, Vrije Universiteit Amsterdam, De Boelelaan 1108, 1081 HZ Amsterdam, The Netherlands
[b] School of Biosciences, University of Kent, Canterbury CT2 7NJ, UK
[c] Mercachem, Kerkenbos 1013, 6546 BB Nijmegen, The Netherlands
[d] Laboratory for Microbiology, Parasitology and Hygiene, Universiteitsplein 1, University of Antwerp, 2610 Wilrijk, Belgium
[e] Institute of Infection, Immunity and Inflammation, University of Glasgow, 120 University Place, Glasgow G12 8TA, UK

ARTICLE INFO

Keywords:
Neglected tropical disease
Human African trypanosomiasis
Trypanosoma brucei phosphodiesterase B1
Structure-based drug discovery
Tetrahydrophthalazinone
Crystal structure

ABSTRACT

Several 3′,5′-cyclic nucleotide phosphodiesterases (PDEs) have been validated as good drug targets for a large variety of diseases. *Trypanosoma brucei* PDEB1 (TbrPDEB1) has been designated as a promising drug target for the treatment of human African trypanosomiasis. Recently, the first class of selective nanomolar TbrPDEB1 inhibitors was obtained by targeting the parasite specific P-pocket. However, these biphenyl-substituted tetrahydrophthalazinone-based inhibitors did not show potent cellular activity against *Trypanosoma brucei (T. brucei)* parasites, leaving room for further optimization. Herein, we report the discovery of a new class of potent TbrPDEB1 inhibitors that display improved activities against *T. brucei* parasites. Exploring different linkers between the reported tetrahydrophthalazinone core scaffold and the amide tail group resulted in the discovery of alkynamide phthalazinones as new TbrPDEB1 inhibitors, which exhibit submicromolar activities versus *T. brucei* parasites and no cytotoxicity to human MRC-5 cells. Elucidation of the crystal structure of alkynamide **8b** (NPD-048) bound to the catalytic domain of TbrPDEB1 shows a bidentate interaction with the key-residue Gln874 and good directionality towards the P-pocket. Incubation of trypanosomes with alkynamide **8b** results in an increase of intracellular cAMP, validating a PDE-mediated effect *in vitro* and providing a new interesting compound series for further studies towards selective TbrPDEB1 inhibitors with potent phenotypic activity.

1. Introduction

Human African trypanosomiasis (HAT), one of the neglected tropical diseases (NTDs), is caused by two members of the trypanosomatids family, i.e. *Trypanosoma brucei (T.b.) rhodesiense* and *T.b. gambiense*.[1] This disease, also called African sleeping sickness, is fatal when left untreated and can have a big socioeconomic effect on rural populations in sub-Saharan Africa.[2] Although the disease was almost eradicated mid-1960s by active screening programs, it re-emerged in the 1980s as a result of discontinued disease surveillance and control programs.[2,3] Five drugs are commonly used for treatment of HAT, but all have major disadvantages including subspecies selectivity, disease stage selectivity, complex administration and toxicity.[4–7] First-stage treatments are generally not effective for the second-stage of the disease, while drugs for the second-stage of the disease are often toxic and require complex administration protocols.[2,4,8] Much of the HAT pharmacopoeia is becoming redundant because of drug resistance, necessitating new control strategies, including new drugs.[6,9,10]

Human 3′,5′-cyclic nucleotide phosphodiesterases (hPDEs) have proven to be successful drug targets for a broad range of diseases, including COPD,[11,12] heart failure[13] and erectile dysfunction.[14] In 2007 Oberholzer *et al.* published *T. brucei* PDEs as potential new targets for the treatment of HAT.[15] The parasite genome encodes four different class I PDE families, PDEA-D, and a simultaneous reduction in the expression of *Trypanosoma brucei* PDEB1 (TbrPDEB1) and TbrPDEB2 with siRNA results in fatal cell cycle defects.[15,16] Furthermore, it was shown

* Corresponding author.
E-mail address: r.leurs@vu.nl (R. Leurs).

https://doi.org/10.1016/j.bmc.2019.06.027
Received 17 September 2018; Received in revised form 21 November 2018; Accepted 14 June 2019

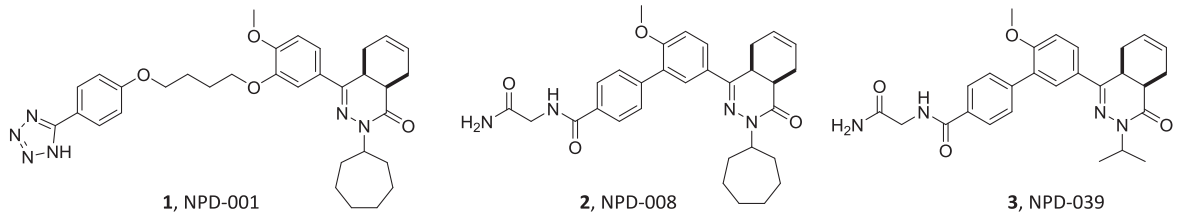

1, NPD-001
TbrPDEB1 pK_i = 8.4
hPDE4 pK_i = 9.2
T. brucei pIC_{50} = 7.7
MRC-5 pCC_{50} = 5.2

2, NPD-008
TbrPDEB1 pK_i = 7.0
hPDE4 pK_i = 6.0
T. brucei pIC_{50} = 5.3
MRC-5 pCC_{50} = 4.4

3, NPD-039
TbrPDEB1 pK_i = 7.0
hPDE4 pK_i = 5.7
T. brucei pIC_{50} = 5.2
MRC-5 pCC_{50} = 4.5

Fig. 1. Previously reported TbrPDEB1 inhibitors.[25,28,32]

that gene silencing by siRNA prevents parasitemia in mice, further demonstrating the potential of TbrPDEB1 and TbrPDEB2 as a target for drugs against HAT.[15]

Several reports have been published about potential starting points for selective inhibitors of this class of parasitic proteins, albeit with mixed results.[17–24] De Koning *et al.* reported a potent nanomolar TbrPDEB1 inhibitor (NPD-001, **1**, Fig. 1), which displays very similar anti-parasitic effects compared to cells treated with TbrPDEB1/2 siRNA, specifically a fatal inability to complete the abscission phase of the cell division.[25] However, the phthalazinone-based scaffold was originally developed as a human PDE4 (hPDE4) inhibitor,[26,27] explaining why NPD-001 and close analogues exhibit sub-nanomolar activities for hPDE4.[24,28] Such a strong PDE4 activity of TbrPDEB1 inhibitors is disqualifying for a potential drug, as hPDE4 inhibition is associated with unacceptable side effects (e.g. emesis, gastro-intestinal disturbance, headache and immune suppression).[24,29–31]

Structural comparison between hPDE4 and TbrPDEB1 reveals the presence of an additional parasite-specific pocket (P-pocket) near the active site, which can be exploited to obtain selective TbrPDEB1 inhibitors.[19,33] Although docking studies had predicted P-pocket occupancy for **1**,[28] the recent elucidation of the X-ray structure of the ligand–protein complex shows the absence of P-pocket interactions by **1**, thereby explaining the lack of TbrPDEB1 selectivity over hPDE4.[32] Recently, we reported the first class of selective TbrPDEB1 inhibitors by rigidifying the catechol linker with a biphenyl system.[32] The two most potent and selective molecules (NPD-008 and NPD-039, **2** and **3** respectively) are shown in Fig. 1. The co-crystal structures of **2** and **3** bound to the catalytic domain of TbrPDEB1 confirmed that the P-pocket is indeed occupied by the glycinamide tail. Unfortunately, both compounds show reduced phenotypic activity against *T. brucei* parasites *in vitro*, halting their further development as anti-*T. brucei* agents and indicating that improvement of the trypanocidal activity is desired.[32]

Herein, we describe the search and discovery of other rigidified molecules based on the same phthalazinone scaffold as **2** and **3**. This new class of TbrPDEB1 inhibitors exhibits submicromolar potency against *T. brucei* and induces a robust, dose-dependent increase in the intracellular cAMP levels of bloodstream form trypanosomes, at concentrations similar to its trypanocidal IC_{50}-value.

2. Results and discussion

2.1. Compound design and inhibitory activity against TbrPDEB1

Since targeting the P-pocket via the biphenyl linker resulted in the expected selectivity of the phthalazinone-based inhibitors **2** and **3** for TbrPDEB1 over hPDE4, further optimisation was started by installing small groups on the biphenyl linker. However, the possibilities to modify the benzamide ring seem very limited, since small changes in size and electron density of the ring dramatically decrease the activity against TbrPDEB1 (Table 1). The minor change of a proton (NPD-008, **2**) to an *ortho* or *meta* fluorine (**4a** and **4d**, respectively) substitution already results in a decrease in potency by at least 0.9 log units. A larger decrease in potency is observed for electron-donating substituents such as methyl and methoxy groups on either position (**4b**, **4c**, **4e** and **4f**). Subtle differences in potency are observed between *ortho*- and *meta*-substitutions, in favour of the modification on the *meta*-position. In addition, the flexibility of the amide bond was reduced by incorporating an isoindole as linker in an attempt to force the substituents to occupy the P-pocket (**5a-c**, Table 1). However, this too resulted in a > 10-fold decrease in potency and adding an ether or amide tail group to N1 (**5b** and **5c**, respectively) did not improve activity either.

As increasing linker size did not improve potency, linker size reductions were investigated. In view of the molecular weight, logP and aqueous solubility of the molecules, it was decided to replace the cycloheptyl substituent of the phthalazinone scaffold with an isopropyl group for this series, as this modification has been shown to yield a small positive effect on the selectivity profile (compare **2** and **3**, Fig. 1). In search for a bioisostere of the phenyl group a thiophene ring was introduced as linker[34], leading to dramatically reduced TbrPDEB1 activity (Table 2), with all thiophene compounds (**6a-e**) showing at least a 100-fold reduction in TbrPDEB1 activity compared to **3**, including **6e**, which represents a direct replacement of the phenyl moiety of **3** with a thiophene. A similar effect was observed when the phenyl ring was replaced by the non-aromatic azetidine group, as none of the azetidines (**7a-d**) display activities below 10 μM.

The results indicate that the vector that defines the accessibility of the P-pocket is not very tolerant to changes. To illustrate the differences in addressing the P-pocket, the unsubstituted thiophene amide and azetidine amide were docked in the crystal structure of TbrPDEB1 ligated with **2** (PDB id: 5G2B) using PLANTS. As illustrated in Fig. 2, a subtle difference in directionality of the linker is observed for the thiophene and azetidine linkers, when compared to **2**. Both analogues bend the carboxamide group towards the protein helix and interact with the conserved residue Gln874, but the interaction seems unproductive as the thiophene-linked amide is in close proximity of the protein and most likely will sterically clash with it.

Therefore, new derivatives with an alkyne functionality were designed that more closely obey the vector as defined by the phenyl-substituent in **2**. A reduction in TbrPDEB1 potency was observed for all alkynamides when compared to **2** (Table 2).

However, modifying the terminal amide (NPD-048, **8b**) with different tail groups gave, as seen with the phenyl linker,[32] a small increase in potency. More flexible tail groups such as a *n*-butyl (**8c**) or furfuryl (**8f**) show a slightly higher activity (pK_i = 6.4 ± 0.1 and 6.3 ± 0.01, respectively) when compared with the more rigid tail groups such as morpholine (**8e**, pK_i = 6.0 ± 0.1). Both observations are in agreement with the previously observed SAR with the biphenyl linker reported by Blaazer *et al.*[32] In contrast to **2**, the highest potency in this new series of TbrPDEB1 inhibitors was not observed with a glycinamide tail (**8g**), but with an *n*-butyl (**8c**) or furfuryl tail (**8f**). Constraining the heteroatoms in an oxazole ring (**8h**) or absence of the amide (**8a**) further reduced inhibitory activity, which could indicate an important function for the amide functionality.

Table 1
Structure-activity relationship of substituted benzamide phthalazinones as TbrPDEB1 inhibitors.

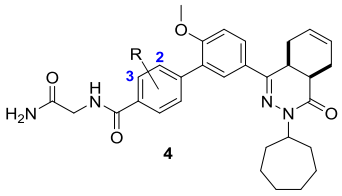

4

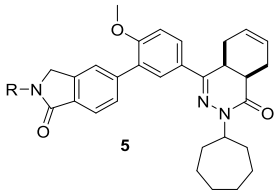

5

#	NPD-	R	pK_i(mean ± S.E.M.)[a]	#	NPD-	R	pK_i (mean ± S.E.M.)[a]
2	008	H	7.0[b]	**5a**	051	H	5.8 ± 0.03
4a	932	2-F	5.7 ± 0.1	**5b**	056	CH_2CH_2OMe	5.9 ± 0.1
4b	948	2-Me	< 5.0	**5c**	052	CH_2CONH_2	5.9 ± 0.01
4c	929	2-OMe	5.1 ± 0.1[c]				
4d	945	3-F	6.1 ± 0.1				
4e	931	3-Me	5.7 ± 0.1				
4f	930	3-OMe	5.2 ± 0.1[c]				

[a] Mean and S.E.M. values of at least 3 independent experiments.
[b] Reported value.[32]
[c] No full dose response curve obtained.

2.2. Biological evaluation

2.2.1. Selectivity alkynamides over hPDE4

To assess the selectivity of the alkynamides as inhibitors for TbrPDEB1 over hPDE4, the inhibitory activity of the alkynamides on hPDE4 was measured (Table 3). In contrast to the previously published selective TbrPDEB1 inhibitor NPD-008 (**2**), the primary carboxamide (**8b**) and the alkynamides **8c–8f** do not display the desired selectivity for inhibition for TbrPDEB1 over human PDE4 (Table 3). Only minor differences in the selectivity index (SI) are observed (range −0.3–0.3). Although the current set of alkynamides does not display the desired selectivity over hPDE4, when compared to the reference inhibitor NPD-001 (**1**) with a SI value of −0.8, the current alkynamide scaffold might offer future options to optimize the selectivity profile via structure-based design (*vide infra*).

2.2.2. Antitrypanosomal activity and cytotoxicity

As mentioned before, the biphenyls **2** or **3** show a reduced potency against the parasite (*T. brucei* pIC_{50} = 5.3 ± 0.2 and 5.2 ± 0.1, respectively) when compared to the potency against TbrPDEB1 (pK_i = 7.0 for both compounds) and an undesirably high cytotoxicity profile for human cells.[32] The alkynamides display submicromolar potencies against TbrPDEB1 and were therefore tested for their antitrypanosomal activity on *T. brucei* parasites, with MRC-5 cells as control for general cytotoxicity towards human cells. The anti-parasitic activity of all the alkynamides was increased when compared to the corresponding biphenyl class (Table 3). The primary carboxamide **8b** (*T. brucei* pIC_{50} 6.0 ± 0.3) is 6-fold more potent than NPD-008, but the cytotoxicity (MRC-5 pCC_{50} = 5.0 ± 0.1) is also increased. Both **8c** and **8f** display an *in vitro* potency against *T. brucei* of 0.6 μM and are non-toxic to human MRC-5 cells at the highest concentration used (64 μM), resulting in an interesting phenotypic profile. Installing a glycinamide tail (**8g**) led to an almost equipotent molecule with decreased antitrypanosomal activity and increased cytotoxicity (*T. brucei* pIC_{50} 5.4 ± 0.01 and MRC-5 pCC_{50} = 5.4 ± 0.02). *N*-Methoxyethyl-substituted alkynamide **8d** was unexpectedly inactive on both cell lines for unknown reasons.

2.2.3. Intracellular cAMP levels

As reported previously, TbrPDEB1 inhibitors such as **1** and **2** are able to increase intracellular cAMP levels in *T. brucei* parasites,[25,32] and we sought to confirm that NPD-048 (**8b**) was likewise acting on the parasite principally through inhibition of the *T. brucei* PDEs. Incubation of *T. brucei* parasites with 3.2 μM and 8 μM of **8b** resulted in highly significant increases in intracellular cAMP levels when compared to untreated control cells (19.8 pmol/5 × 10^6 cells ($P < 0.01$) and 311 pmol/5 × 10^6 cells ($P < 0.001$) *vs.* 6.66 pmol/5 × 10^6 cells, respectively).

2.3. Crystal structures

In order to investigate the binding mode of the alkynamides, we determined the co-crystal structures of the TbrPDEB1 and hPDE4D catalytic domains in complex with **8b**, at 2.10 and 2.16 Å resolution, respectively (Fig. 3A, B). The PDE inhibitor binds in an almost identical manner to both catalytic sites, maintaining the key hydrophobic interactions in the hydrophobic clamp region and a hydrogen bond interaction with the conserved Gln874, all mediated through its anisole moiety.

Furthermore, the carbonyl of the alkynamide creates a second hydrogen bond interaction with the conserved Gln874. The co-crystal structures clearly show that the alkynamide inhibitor **8b** engages identically with both enzymes (Fig. 3C). Moreover, the inability of **8b** to reach the P-pocket explains its lack of selectivity towards TbrPDEB1. The alignment of the binding pose of **8b** with the binding pose of **2** in TbrPDEB1 (Fig. 3D) shows that **8b** adopts a binding mode which is slightly rotated to facilitate the double interaction with Gln874, positioning the carboxamide in front of the P-pocket. This positioning provides an interesting opportunity for optimization of the alkynamide phthalazinone scaffold. Further exploration by extension of the tail group to target the P-pocket is currently ongoing.

2.4. Synthesis

The racemic *cis*-cycloheptyl tetrahydrophthalazinone scaffold (building block **9**) was synthesized as described previously.[27,28,32] Derivatives **4** and **5** were synthesized via two different synthetic pathways. Firstly, a Suzuki reaction of **9** with the corresponding phenylboronic acid was performed to obtain carboxylic acid **10a** and methyl ester **10b**, which was hydrolyzed to carboxylic acid **10c** in quantitative yield (Scheme 1). The glycinamide tail was introduced by an amide coupling using EDC/HOAt to afford **4b** and **4d**. Secondly, building block **9** was converted to pinacol boronate ester **11** in moderate yield and a subsequent Suzuki reaction with the corresponding

Table 2
Structure-activity relationship of phthalazinones with reduced linker size against TbrPDEB1.

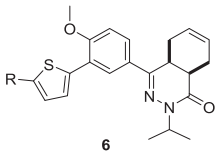

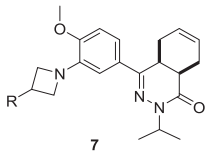

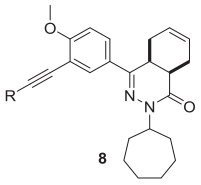

#	NPD-	R	pK_i (mean ± S.E.M.)[a]	#	NPD-	R	pK_i (mean ± S.E.M.)[a]
2	008	–	7.0[b]	**8a**	064	H	5.4 ± 0.1[c]
3	039	–	7.0[b]	**8b**	048		6.2 ± 0.02
6a	1030		5.0 ± 0.06[c]	**8c**	055	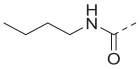	6.4 ± 0.02
6b	1027	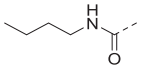	< 5.0	**8d**	050	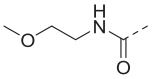	6.1 ± 0.1
6c	092	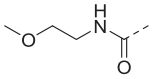	< 5.0	**8e**	054	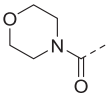	6.0 ± 0.1
6d	1029	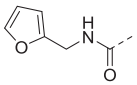	< 5.0	**8f**	053	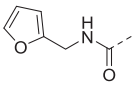	6.3 ± 0.01
6e	1028	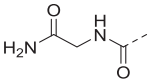	< 5.0	**8g**	046	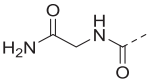	6.2 ± 0.1
7a	1259		< 5.0	**8h**	065		< 5.0
7b	1256	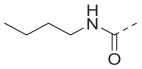	< 5.0				
7c	1258	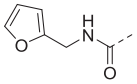	< 5.0				
7d	1257	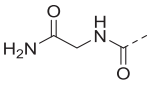	< 5.0				

[a] Mean and S.E.M. values of at least 3 independent experiments.
[b] Reported values.[32]
[c] No full dose response curve obtained.

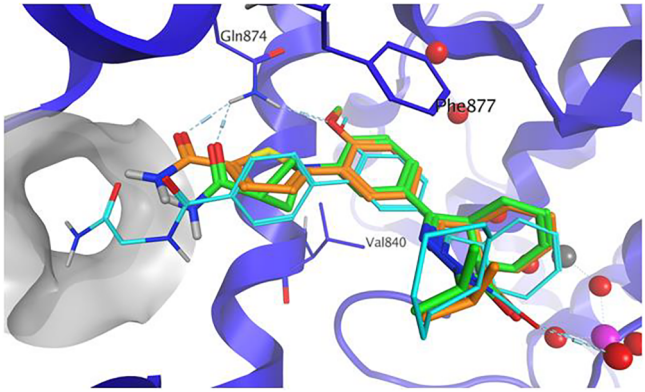

Fig. 2. Binding prediction of the phthalazinones with a thiophene amide (orange) and azetidine amide (green) linker superposed on the X-ray structure of **2** (cyan) co-crystallized in the catalytic domain of TbrPDEB1 (modelled using the PLANTS software package). Key residues, active site water molecules and metals are shown for clarity. (For interpretation of the references to colour in this figure legend, the reader is referred to the web version of this article.)

Table 3
Selectivity data for the synthesized alkynamides and their phenotypical activities (mean ± S.E.M).

	pK_i-value				
#	TbrPDEB1	hPDE4	ΔpK_i	*T. brucei* (pIC_{50})	MRC-5 (pCC_{50})
2	7.0[a]	6.0[a]	1.0	5.3 ± 0.2[a]	4.4[a]
3	7.0[a]	5.7[a]	1.3	5.2 ± 0.1[a]	4.5[a]
8b	6.2 ± 0.02	6.5 ± 0.2	−0.3	6.0 ± 0.3	5.0 ± 0.1
8c	6.4 ± 0.02	6.2 ± 0.2	0.2	6.2 ± 0.3	< 4.2
8d	6.1 ± 0.1	5.8 ± 0.3	0.3	< 4.2	< 4.2
8f	6.3 ± 0.01	6.4 ± 0.1	−0.1	6.2 ± 0.1	4.3 ± 0.2
8g	6.2 ± 0.1	ND	–	5.4 ± 0.01	5.4 ± 0.02

[a] Reported values.[32]

arylbromide **12a-d** (synthesized from the corresponding 4-bromobenzoic acid and glycinamide using EDC/HOAt) led to the desired compounds **4a**, **4c**, **4e** and **4f**. Isoindolinones (**5a-c**) were synthesized using a Suzuki reaction followed by an alkylation using the corresponding alkyl bromide (Scheme 1).

Incorporation of the alkyne functionality to carboxylic acid **13** could be achieved in a Sonogashira reaction of propiolic acid with **9** (Scheme

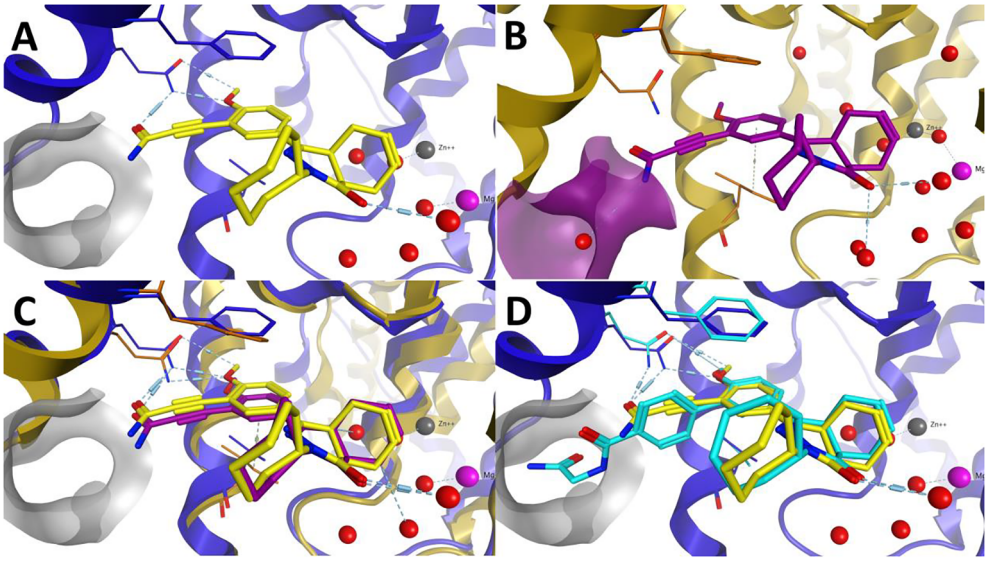

Fig. 3. A) X-ray structure of **8b** in TbrPDEB1 (PDB id: 6FTM) and B) hPDE4D (PDB id: 6FTW). A molecular surface of the P-pocket region in TbrPDEB1 (grey) and hPDE4D (purple) is displayed to highlight the structural differences between both enzymes. C) Overlay of **8b** in TbrPDEB1 (blue) and hPDE4D (dark yellow). D) Overlay of **8b** and NPD-008 (**2**) in TbrPDEB1. Key residues for interaction with the substrate are shown and active site water molecules are shown as red spheres. Binding site metals zinc and magnesium are displayed as grey and magenta spheres, respectively. (For interpretation of the references to colour in this figure legend, the reader is referred to the web version of this article.)

2). However, since **13** was found to slowly degrade over time, it was decided to use the crude material in a subsequent reaction with glycinamide to obtain **8g**, albeit in an extremely low yield. An alternative route towards the alkynamides avoiding the unstable carboxylic acid **13** involved synthesizing methyl ester **14** from pinacol boronate **11** (Scheme 1) in moderate yield, followed by an amidation in absence (for **8b**) or presence (for **8c-f**) of the Lewis acid trimethylaluminium. Unfortunately, synthesis of alkynamide **8g** was unsuccessful using this procedure. The primary alkyne **8a** was synthesized via a Sonogashira reaction with TMS-acetylene followed by deprotection of **15** with NaOH, both in high yield. The resulting alkyne in **8a** was converted into aldehyde **16** and used subsequently in the Van Leusen oxazole synthesis to obtain **8h**.

The racemic *cis*-isopropyl tetrahydrophthalazinone building block (**17**) was synthesized using the same procedure as described previously. Building block **17** was used in a Suzuki reaction using 5-

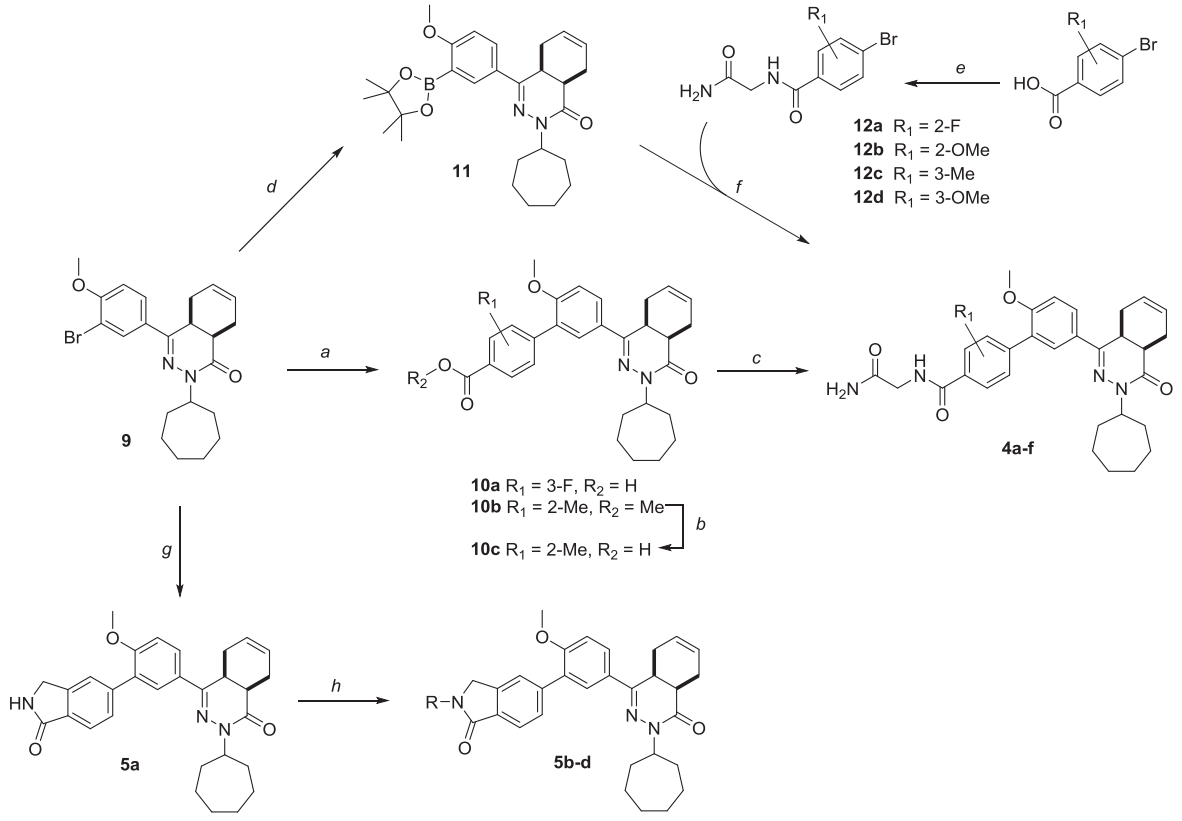

Scheme 1. Reagents and conditions: a) corresponding boronic acid, $PdCl_2$(dppf), Na_2CO_3, DME, H_2O, 100 °C, 5 h, **10a**: 46%, **10b**: 39%; b) NaOH, THF, MeOH, 50 °C, 16 h, 98%; c) For **4b** and **4d**: glycinamide.HCl, EDC.HCl, HOAt, Et_3N, DCM, rt, 1 h, **4b**: 83%, **4d**: 23%; d) Bis(pinacolato)diboron, $PdCl_2$(dppf), KOAc, dioxane, reflux, 2.5 h, 28%; e) glycinamide.HCl, EDC.HCl, HOAt, Et_3N, DCM, rt, overnight, 47–59%; f) For **4a**, **4c**, **4e** and **4f**: corresponding bromide, $PdCl_2$(dppf), Na_2CO_3, DME, H_2O, 100 °C, 5 h, 27–57%; g) 5-(4,4,5,5-tetramethyl-1,3,2-dioxaborolan-2-yl)isoindolin-1-one, $PdCl_2$(dppf), Na_2CO_3, DME, H_2O, 100 °C, 5 h, 73%; h) 1) NaH, DMF, rt, 30 min; 2) R-Br, rt, 1.5 h, 14–27%.

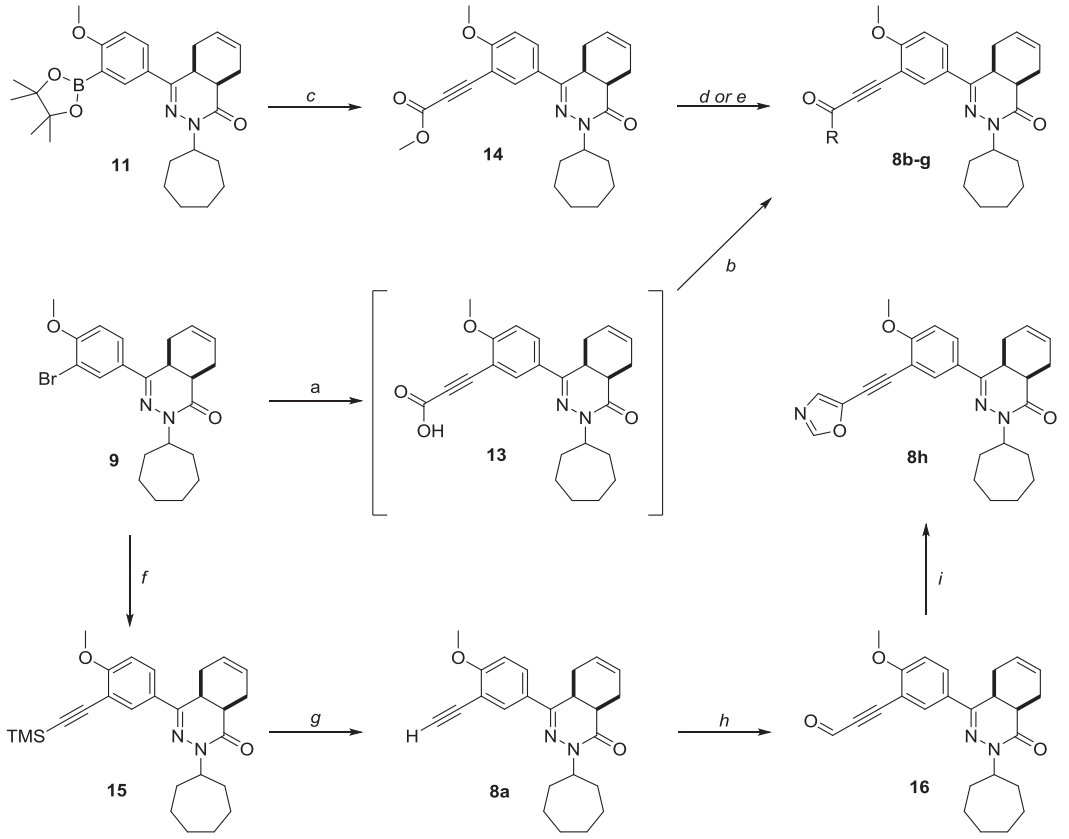

Scheme 2. Reagents and conditions: a) Propiolic acid, $Pd(PPh_3)_2Cl_2$, dppb, DBU, DMSO, 50 °C, 15 h, used crude; b) For **8g**: glycinamide.HCl, EDC.HCl, HOAt, Et_3N, DCM, rt, 30 h, 1% over 2 steps; c) Methyl propiolate, $Pd(OAc)_2$, K_2CO_3, AgO, 70 °C, 3 h, 53%; d) For **8b**: NH_3, MeOH, rt, 2 h, 89%; e) For **8c-8f**: corresponding amine, $AlMe_3$, PhMe, 50 °C, 1 d, 16–37%; f) Ethynyltrimethylsilane, $Pd(PPh_3)_2Cl_2$, CuI, TEA, 80 °C, 3 h, 80%; g) NaOH, MeOH, H_2O, rt, 2 h, 91% yield; h) 1) *n*-BuLi, THF, −78 °C, 30 min, 2) DMF, −78 °C, 1.5 h, 69%; i) 1-((isocyanomethyl)sulfonyl)-4-methylbenzene, K_2CO_3, MeOH, reflux, 1.5 h, 47%.

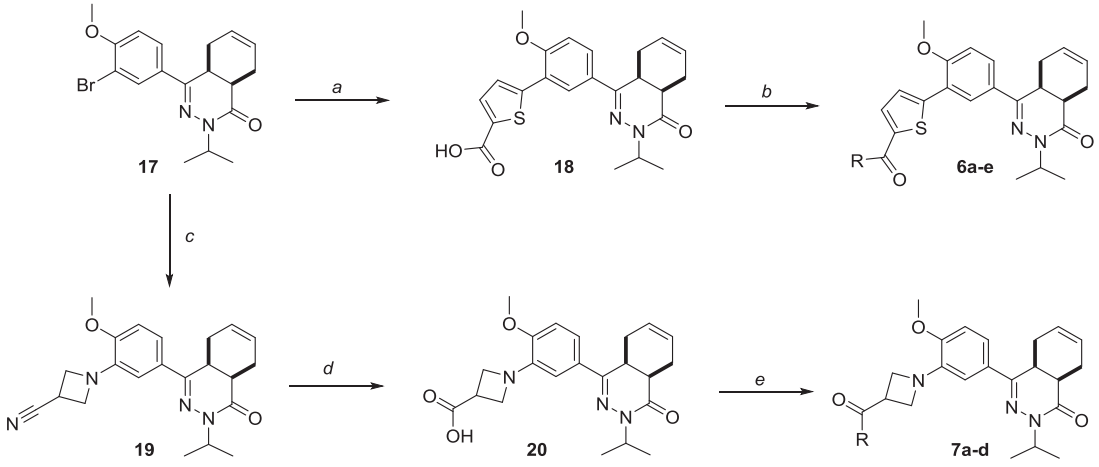

Scheme 3. Reagents and conditions: *a*) 5-boronothiophene-2-carboxylic acid, $PdCl_2(dppf)$, Na_2CO_3, DME, H_2O, reflux, 5 h, 73%; *b*) Corresponding amine, EDC.HCl, HOBt, Et_3N, DCM, rt, 1 d, 15–76% yield; *c*) azetidine-3-carbonitrile.HCl, Cs_2CO_3, $Pd(OAc)_2$, XPhos, PhMe, 100 °C, 3 d, 46%; *d*) NaOH, H_2O, EtOH, 75 °C, 1 d, 47%; *e*) corresponding amine, EDC.HCl, HOBt, Et_3N, DCM, rt, 1 d, 31–70%.

boronothiophene-2-carboxylic acid, followed by an amide coupling to obtain **6a-e** (Scheme 3). The azetidine linker was introduced using a Buchwald-Hartwig cross coupling reaction with 3-cyanoazetidine to obtain nitrile **19**. The nitrile was hydrolyzed using NaOH and the formed carboxylic acid **20** was coupled to various amines using EDC/HOBt to obtain azetidines **7a-d**.

3. Conclusion

A class of tetrahydrophthalazinone-based TbrPDEB1 inhibitors with an alkynamide linker was identified as potent TbrPDEB1 inhibitors with good potency against *T. brucei* parasites and an interesting cytotoxicity profile. Alkynamide **8c** (NPD-055) inhibits TbrPDEB1 *in vitro,* shows a

submicromolar trypanocidal activity (IC_{50} = 0.6 μM) against *T. brucei* parasites and displays no cytotoxicity versus human MRC-5 cells (CC_{50} > 64 μM). The alkynamide **8b** (NPD-048) was co-crystallized in the catalytic domain of TbrPDEB1, showing a bidentate interaction of **8b** with the key residue Gln874 in the active site. Moreover, this bidentate interaction positions the carboxamide of **8b** in close proximity to the P-pocket of TbrPDEB1. The alkynamide **8b** is able to raise intracellular cAMP levels in living *T. brucei* parasites, supporting a PDE-mediated mode of action *in vitro*.

4. Experimental

4.1. Protein production

Cloning, expression and purification of recombinant TbrPDEB1 and hPDE4D catalytic domains were performed as previously described.[32]

4.2. Crystallisation, data collection and structure determination of inhibitor complexes

TbrPDEB1 and hPDE4D catalytic domain crystals were grown in 24 well XRL plates (Molecular Dimensions) by vapor diffusion hanging drop technique, typically maintaining a protein to crystallisation solution ratio of 1:1 and a reservoir volume of 500 μL. Crystals of TbrPDEB1 were obtained in a condition containing 20% PEG 3350, 400 mM sodium formate, 300 mM guanidine and 100 mM MES pH 6.5 at 4 °C and were complexed with NPD-048 by soaking in the crystal growth solution containing 15 mM of the inhibitor for a period of 48 h. The soaked crystals were then cryo protected, mounted on CryoLoop (Hampton Research) or LithoLoops (Molecular Dimensions) and vitrified in liquid nitrogen for data collection.

Crystals of hPDE4D catalytic domain were obtained in a condition containing 24% PEG 3350, 30% ethylene glycol and 100 mM HEPES pH 7.5 at 19 °C. Crystals were soaked with NPD-048 and archived in a way similar to that of TbrPDEB1.

X-ray diffraction data were collected at Diamond Light Source (Didcot, Oxfordshire, UK) beam lines I04 and I04-1 at 100 K using Pilatus 6 M-F detector (Dectris, Baden, Switzerland) and were processed with XIA2 pipeline,[35] which incorporates XDS[36] and AIMLESS,[37] or were integrated using iMOSFLM[38] and reduced using POINTLESS, AIMLESS and TRUNCATE, all of which are part of CCP4.[39]

Structure of TbrPDEB1 and hPDE4D complexes with NPD-048 were determined by molecular replacement using CCP4 suite program PHASER[40] that utilised respective apo models (TbrPDEB1, PDB id: 4I15; hPDE4D, PDB id: 3SL3) as search templates. Stereochemical description of NPD-048 was generated by ACEDRG available within the CCP4 package[39] and ligand fitting and model adjustment were carried out in COOT[41] followed by maximum likelihood refinement with REFMAC[42]. Data processing and refinement statistics are given in Table 4. Structural figures were prepared with PYMOL.[43] Coordinates of the structures have been deposited to the RCSB Protein Data Bank with following accession codes: 6FTM (TbrPDEB1–NPD-048) and 6FTW (hPDE4D–NPD-048).

4.2.1. Accession codes

The coordinates of the crystal structures have been deposited to the RCSB Protein Data Bank under the following accession codes: 6FTM (TbrPDEB1–NPD-048); 6FTW (hPDE4D–NPD-048); The authors will release the atomic coordinates and experimental data upon article publication.

4.3. Phosphodiesterase activity assays

The PDELight™ HTS cAMP phosphodiesterase Kit (Lonza, Walkersville, USA) was used. The assay was performed at 25 °C in non-binding, low volume 384 wells plates (Corning, Kennebunk, ME, USA).

Table 4
Data collection and refinement statistics for NPD-048 bound TbrPDEB1 and hPDE4D catalytic domain crystals.

		TbrPDEB1	hPDE4D
Data collection			
Space group		*C* 1 2 1	*P* 2_1 2_1 2_1
Molecule/a.s.u Cell dimensions		2	4
	a, *b*, *c* (Å)	149.05, 114.73, 63.80	99.14, 111.43, 160.06
α,β,γ(°)		90, 109.43, 90	90, 90, 90
Resolution (Å)		70.28–2.10 (2.16–2.10)*	65.00–2.16 (2.22–2.16)
R_{merge}		0.103 (0.475)	0.085 (1.063)
$I/\sigma I$		7.1 (2.3)	14.5 (1.7)
CC(1/2)		0.992 (0.603)	0.999 (0.623)
Completeness (%)		99.8 (99.9)	99.9 (99.8)
Redundancy		3.1 (2.8)	6.7 (6.6)
Refinement			
Resolution (Å)		2.10	2.16
No. reflections		55,845 (4137)	90,714 (6591)
R_{work}/R_{free}		0.157/0.198	0.182/0.233
No. atoms			
	Protein	5272	10,561
	Ligand	62	124
	Water	327	551
B-factors			
	Protein	31.85	48.37
	Ligand	37.11	59.31
	Water	39.96	47.36
R.m.s. deviations			
	Bond lengths (Å)	0.019	0.017
	Bond angles (°)	1.834	1.761
PDB accession no.		6FTM	6FTW
PDB ligand code		E6Z	E6Z

Data were collected from one crystal in each case.
* Values in parentheses are for highest-resolution shell.

PDE activity measurements (TbrPDEB1_CD; K_m 3.45 μM, hPDE4B_CD; K_m 13.89 μM) were made in 'stimulation buffer' (50 mM Hepes, 100 mM NaCl, 10 mM MgCl, 0.5 mM EDTA, 0.05 mg/mL BSA, pH 7.5). Single concentration measurements were made at 10 μM inhibitor concentration (triplo measurements/assay, n = 2). Dose response curves were made in the range 100 μM–10 pM (triplo measurements/assay, n = 3). Compounds were diluted in DMSO (final concentration 1%). Inhibitor dilutions (2.5 μL) were transferred to the 384 wells plate, 2.5 μL PDE in stimulation buffer was added and mixed, 5 μL cAMP (at 2 × K_m up to 20 μM) is added and the assay mixture was incubated for 20 min at 300 rpm. The reaction was terminated by addition of 5 μL Lonza Stop Buffer supplemented with 10 μM NPD-001. Then 5 μL of Lonza Detection reagent (diluted to 80% with reaction buffer) was added and the reaction incubated for 10 min at 300 rpm. Luminescence was read with a Victor3 luminometer using a 0.1 s/well program.

RLUs were measured in comparison to the DMSO-only control, NPD-001 always was taken along as positive control as a PDE inhibitor. The K_i values of the inhibitors analyzed are represented as the mean of at least three independent experiments with the associated standard error of the mean (S.E.M.) as indicated. Due to solubility issues, we were not able to determine full dose response curves for all compounds; K_i values for such inhibitors were obtained by curve fitting (Graphpad Prism 7.0) and the assumption of full inhibition to a level of inhibition by NPD-001.

4.4. Phenotypic cellular assays

For the cellular assays, the following reference drugs were used as positive controls: suramin (Sigma-Aldrich, Germany) for *T. brucei*

(pIC_{50} = 7.4 ± 0.2, n = 5), and tamoxifen (Sigma-Aldrich, Germany) for MRC-5 cells (pIC_{50} = 5.0 ± 0.1, n = 5). All compounds were tested at five concentrations (64, 16, 4, 1 and 0.25 μM) to establish a full dose-titration and determination of the IC_{50} and CC_{50}, data are represented as the mean of duplicate experiments ± S.E.M. The final concentration of DMSO did not exceed 0.5% in the assays.

Antitrypanosomal cellular assay. *T.b. brucei* Squib-427 strain (suramin-sensitive) was cultured at 37 °C and 5% CO_2 in HMI-9 medium, supplemented with 10% fetal calf serum (FCS). Approximately 1.5×10^4 trypomastigotes were added to each well and parasite growth was assessed after 72 h at 37 °C by adding resazurin. Viability was assessed fluorimetrically 24 h after the addition of resazurin. Fluorescence was measured (excitation 550 nm, emission 590 nm) and the results were expressed as percentage reduction in viability compared to control.

MRC-5 cytotoxicity cellular assay. MRC-5 SV2 cells, originally from a human diploid lung cell line, were cultivated in MEM, supplemented with L-glutamine (20 mM), 16.5 mM sodium hydrogen carbonate and 5% FCS. For the assay, 10^4 MRC-5 cells/well were seeded onto the test plates containing the pre-diluted sample and incubated at 37 °C and 5% CO_2 for 72 h. Cell viability was assessed fluorimetrically 4 h after the of addition of resazurin. Fluorescence was measured (excitation 550 nm, emission 590 nm) and the results were expressed as percentage reduction in cell viability compared to control.

4.5. Intracellular cAMP assay

Quantification of intracellular cAMP was performed exactly as described previously, using the Direct Cyclic AMP Enzyme Immunoassay kit (Assay Designs).[25] Briefly, bloodstreams form trypanosomes were seeded at a density of 2×10^6 cells/mL in the log phase and incubated at 37 °C and 5% CO_2 overnight followed by incubation with or without (negative control) potential PDE inhibitors at 2 × and 5 × IC_{50}-values. After 4 h, 5×10^6 cells/mL were counted for both treated and control, transferred to microfuge tubes and centrifuged at 2000*g* for 10 min at 4 °C in a Heraeus Biofuge centrifuge. The cell pellet was resuspended in 100 μL 0.1 M hydrochloric acid, placed on ice for 20 min, followed by centrifugation at 12,000 rpm for 10 min. The supernatant was stored at −20 °C until assayed in duplicate using the Assays Design immunoassay kit, following the manufacturer's instructions. All experiments were performed at least three times independently.

4.6. Chemistry

4.6.1. General

All reagents and solvents were obtained from commercial suppliers and were used as received. All reactions were magnetically stirred and carried out under an inert atmosphere. Reaction progress was monitored using thin-layer chromatography (TLC) and LC-MS analysis. LC-MS analysis was performed on a Shimadzu LC-20AD liquid chromatograph pump system, equipped with an Xbridge (C18) 5 μm column (50 mm, 4.6 mm), connected to a Shimadzu SPD-M20A diode array detector, and MS detection using a Shimadzu LC-MS-2010EV mass spectrometer. The LC-MS conditions were as follows: solvent A (water with 0.1% formic acid) and solvent B (MeCN with 0.1% formic acid), flow rate of 1.0 mL/min, start 5% B, linear gradient to 90% B in 4.5 min, then 1.5 min at 90% B, then linear gradient to 5% B in 0.5 min, then 1.5 min at 5% B; total run time of 8 min. Silica gel column chromatography was carried out with automatic purification systems using the indicated eluent. Reversed phase column purification was performed on Grace Davison iES system with C18 cartridges (60 Å, 40 μm) using the indicated eluent. Nuclear magnetic resonance (NMR) spectra were recorded as indicated on a Bruker Avance 500 (500 MHz for ^1H and 125.8 MHz for ^{13}C) instrument equipped with a Bruker CryoPlatform, or on a Bruker DMX300 (300 MHz for ^1H) or a Bruker Biospin (400 MHz for ^1H). Chemical shifts (δ in ppm) and coupling constants (*J* in Hz) are reported with residual solvent as internal standard (δ ^1H NMR: $CDCl_3$ 7.26; DMSO-d_6 2.50; δ ^{13}C NMR: $CDCl_3$ 77.16; DMSO-d_6 39.52). Abbreviations used for ^1H NMR descriptions are as follows: s = singlet, d = doublet, t = triplet, q = quintet, hept = heptet dd = doublet of doublets, dt = doublet of triplets, tt = triplet of triplets, m = multiplet, app d = apparent doublet, br = broad signal. Exact mass measurements (HRMS) were performed on a Bruker micrOTOF-Q instrument with electrospray ionization (ESI) in positive ion mode and a capillary potential of 4500 V. Microwave reactions were carried out in a Biotage Initiator$^+$ using sealed microwave vials. Systematic names for molecules were generated with ChemBioDraw Ultra 14.0.0.117 (PerkinElmer, Inc.). The reported yields refer to isolated pure products and are not optimized. The purity, reported as the LC peak area % at 254 nm, of all final compounds was ≥95% based on LC-MS. All compounds are isolated as a racemic mixture of *cis*-enantiomers.

4.6.2. Synthetic procedures

Building block **9** and **17** were prepared as described elsewhere.[27,28,32] All other compounds were prepared as described below.

*4.6.2.1. 5′-(cis-3-Cycloheptyl-4-oxo-3,4,4a,5,8,8a-hexahydrophthalazin-1-yl)-3-fluoro-2′-methoxy-[1,1′-biphenyl]-4-carboxylic acid (**10a**).* To an argon purged solution of **9** (0.50 g, 1.7 mmol) and methyl 2-fluoro-4-(4,4,5,5-tetramethyl-1,3,2-dioxaborolan-2-yl)benzoate (0.40 g, 2.0 mmol) in DME (8 mL) was added aq. Na_2CO_3 (1.7 M, 2.0 mL) and $PdCl_2$(dppf) (53 mg, 60 μmol). The reaction mixture was stirred and heated by microwave irradiation at 100 °C for 1 h. The reaction mixture was diluted with water (20 mL) and washed with EtOAc (60 mL). The aqueous phase was acidified to ~pH 1 with aq. HCl and extracted with EtOAc (3 × 50 mL). The combined organic phases were washed with water (40 mL), brine (40 mL), dried over Na_2SO_4, filtered and concentrated. The residue was purified on a reverse phase silica gel column eluting with MeCN/H_2O + 0.1% formic acid (gradient, 5–95%) to afford **10a** as a yellow solid (268 mg, 46%).

^1H NMR (300 MHz, $CDCl_3$): *δ* 8.09 (t, *J* = 8.1 Hz, 1H), 7.88–7.81 (m, 1H), 7.77 (s, 1H), 7.47–7.36 (m, 2H), 7.07 (d, *J* = 8.7 Hz, 1H), 5.84–5.63 (m, 2H), 4.89–4.75 (m, 1H), 3.89 (s, 3H), 3.39–3.25 (m, 1H), 3.09–2.95 (m, 1H), 2.75 (t, *J* = 5.4 Hz, 1H), 2.29–1.39 (m, 15H).

*4.6.2.2. Methyl 5′-(cis-3-cycloheptyl-4-oxo-3,4,4a,5,8,8a-hexahydrophthalazin-1-yl)-2′-methoxy-2-methyl-[1,1′-biphenyl]-4-carboxylate (**10b**).* This compound was prepared from **9** (500 mg, 1.16 mmol) and methyl 3-methyl-4-(4,4,5,5-tetramethyl-1,3,2-dioxaborolan-2-yl) benzoate (384 mg, 1.39 mmol) as described for **10a**. The title compound was obtained as a white solid (228 mg, 39%).

^1H NMR (300 MHz, $CDCl_3$): *δ* 7.96–7.90 (m, 2H), 7.86 (dd, *J* = 8.7 Hz, 2.4 Hz, 1H), 7.56 (d, *J* = 2.4 Hz, 1H), 7.29 (d, *J* = 7.8 Hz, 1H), 7.03 (d, *J* = 8.7 Hz, 1H), 5.81–5.61 (m, 2H), 4.85–4.74 (m, 1H), 3.93 (s, 3H), 3.81 (s, 3H), 3.33–3.23 (m, 1H), 3.06–2.95 (m, 1H), 2.73 (t, *J* = 6.0 Hz, 1H), 2.20 (s, 3H), 2.18–1.41 (m, 15H).

*4.6.2.3. 5′-(cis-3-Cycloheptyl-4-oxo-3,4,4a,5,8,8a-hexahydrophthalazin-1-yl)-2′-methoxy-2-methyl-[1,1′-biphenyl]-4-carboxylic acid (**10c**).* To a solution of **10b** (228 mg, 0.46 mmol) in MeOH (5 mL) and THF (12 mL) was added an aqueous solution of NaOH (2.0 M, 3.6 mL) and the reaction mixture was stirred overnight at 50 °C. The reaction mixture was cooled to rt, acidified with aq. HCl (4 M) and extracted with EtOAc (3 × 20 mL). The combined organic phases were washed with water (15 mL), brine (15 mL), dried over Na_2SO_4, filtered and concentrated to obtain **10c** as a white solid (219 mg, 98%).

^1H NMR (300 MHz, $CDCl_3$): *δ* 8.08–7.98 (m, 2H), 7.88 (dd, *J* = 8.7 Hz, 2.4 Hz, 1H), 7.58 (d, *J* = 2.4 Hz, 1H), 7.34 (d, *J* = 7.8 Hz, 1H), 7.05 (d, *J* = 8.7 Hz, 1H), 5.83–5.62 (m, 2H), 4.86–4.75 (m, 1H), 3.83 (s, 3H), 3.35–3.24 (m, 1H), 3.08–2.95 (m, 1H), 2.75 (t, *J* = 6.3 Hz, 1H), 2.23 (s, 3H), 2.19–1.42 (m, 15H).

*4.6.2.4. cis-2-Cycloheptyl-4-(4-methoxy-3-(4,4,5,5-tetramethyl-1,3,2-dioxaborolan-2-yl)phenyl)-4a,5,8,8a-tetrahydrophthalazin-1(2H)-one (**11**).* To an argon-purged solution of **9** (1.7 g, 3.8 mmol) in 1,4-dioxane (30 mL) was added KOAc (0.75 g, 7.7 mmol), bis(pinacolato)diboron (1.1 g, 4.2 mmol) and $PdCl_2$(dppf) (0.14 g, 0.19 mmol). The mixture was heated to reflux for 2.5 h. The reaction mixture was diluted with DCM (150 mL) and the mixture was washed with water (2 × 100 mL) and brine (100 mL). The organic phase was dried over Na_2SO_4, filtered and concentrated. The residue was purified on a silica gel column eluting with EtOAc/*n*-heptane (gradient, 10–30%) to afford **11** as a white solid (0.5 g, 28%).

^{1}H-NMR (400 MHz, $CDCl_3$): δ 8.01–7.95 (m, 2H), 6.92 (d, J = 8.7 Hz, 1H), 5.83–5.63 (m, 2H), 4.89–4.75 (m, 1H), 3.88 (s, 3H), 3.35 (q, J = 5.8 Hz, 1H), 3.03 (app d, 1H), 2.70 (t, J = 5.7 Hz, 1H), 2.23–1.21 (m, 24H).

LC-MS (ESI): t_R = 2.54 min, area: > 95%, *m/z* 479 $[M+H]^+$.

*4.6.2.5. N-(2-Amino-2-oxoethyl)-4-bromo-3-fluorobenzamide (**12a**).* To a solution of 4-bromo-3-fluorobenzoic acid (500 mg, 2.28 mmol) in DCM (25 mL) was added DIPEA (0.63 mL, 3.65 mmol), glycinamide.HCl (252 mg, 2.28 mmol), EDC.HCl (481 mg, 2.51 mmol) and HOAt (31 mg, 0.23 mmol). The reaction mixture was stirred overnight at rt and poured into water (120 mL). The solids were isolated by vacuum filtration to obtain **12a** as a white solid (338 mg, 58%).

^{1}H NMR (300 MHz, DMSO-d_6): δ 8.87 (t, J = 6.0 Hz, 1H), 7.88–7.81 (m, 2H), 7.68 (dd, J = 8.4 Hz, 2.1 Hz, 1H), 7.41 (br, 1H), 7.06 (br, 1H), 3.82 (d, J = 6.0 Hz, 2H).

*4.6.2.6. N-(2-Amino-2-oxoethyl)-4-bromo-3-methoxybenzamide (**12b**).* This compound was prepared from 4-bromo-3-methoxybenzoic acid (500 mg, 2.16 mmol) and glycinamide.HCl (300 mg, 2.74 mmol) as described for **12a**. The title compound was obtained as a white solid (385 mg, 59% yield).

^{1}H NMR (300 MHz, DMSO-d_6): δ 8.78 (t, J = 5.7 Hz, 1H), 7.70 (d, J = 8.1 Hz, 1H), 7.57 (d, J = 1.8 Hz, 1H), 7.46–7.35 (m, 2H), 7.05 (br, 1H), 3.92 (s, 3H), 3.81 (d, J = 6.0 Hz, 2H).

*4.6.2.7. N-(2-Amino-2-oxoethyl)-4-bromo-2-methylbenzamide (**12c**).* This compound was prepared from 4-bromo-2-methylbenzoic acid (500 mg, 2.33 mmol) and glycinamide.HCl (514 mg, 4.65 mmol) as described for **12a**. The title compound was obtained as a light-brown solid (300 mg, 47%).

^{1}H NMR (300 MHz, DMSO-d_6): δ 8.46–8.36 (m, 1H), 7.52–7.29 (m, 4H), 7.02 (br, 1H), 3.78 (d, J = 6.0 Hz, 2H), 2.35 (br, 3H).

*4.6.2.8. N-(2-Amino-2-oxoethyl)-4-bromo-2-methoxybenzamide (**12d**).* This compound was prepared from 4-bromo-2-methoxybenzoic acid (500 mg, 2.16 mmol) and glycinamide.HCl (478 mg, 4.33 mmol) as described for **12a**. The title compound was obtained as a white solid (350 mg, 55%).

^{1}H NMR (300 MHz, DMSO-d_6): δ 8.52–8.42 (m, 1H), 7.80 (d, J = 8.1 Hz, 1H), 7.43–7.34 (m, 2H), 7.27 (dd, J = 8.1 Hz, 1.8 Hz, 1H), 7.10 (br, 1H), 3.95 (s, 3H), 3.88 (d, J = 6.0 Hz, 2H).

*4.6.2.9. N-(2-Amino-2-oxoethyl)-5′-(cis-3-cycloheptyl-4-oxo-3,4,4a,5,8,8a-hexahydrophthalazin-1-yl)-2-fluoro-2′-methoxy-[1,1′-biphenyl]-4-carboxamide (**4a**).* To an argon purged solution of **11** (0.20 g, 0.42 mmol) and **12a** (0.12 g, 0.42 mmol) in DME (3.2 mL) was added an aqueous solution of Na_2CO_3 (1.6 M, 0.40 mL) and $PdCl_2$(dppf) (19 mg, 0.02 mmol). The reaction mixture was stirred at 100 °C for 1 h. The reaction mixture was diluted with water (8 mL) and washed with EtOAc (25 mL). The water phase was acidified to ~pH 5 with HCl (aq. 2 M) and extracted with EtOAc (4 × 20 mL). The combined organic phases were washed with water (3 × 20 mL), brine (20 mL), dried over Na_2SO_4 and concentrated. The residue was purified on a reverse phase silica gel column eluting with MeCN/H_2O + 0.1% formic acid (gradient, 5–95%) to afford **4a** as a light yellow solid (62 mg, 27%).

^{1}H NMR (500 MHz, DMSO-d_6): δ 8.84 (t, J = 6.0 Hz, 1H), 7.93 (dd, J = 8.7, 2.2 Hz, 1H), 7.81–7.71 (m, 3H), 7.51 (t, J = 7.6 Hz, 1H), 7.43 (s, 1H), 7.23 (d, J = 8.8 Hz, 1H), 7.09 (s, 1H), 5.72–5.58 (m, 2H), 4.67 (tt, J = 8.8, 4.8 Hz, 1H), 3.83 (d, J = 5.9 Hz, 2H), 3.80 (s, 3H), 3.47 (dt, J = 11.6, 5.8 Hz, 1H), 2.79 (t, J = 6.2 Hz, 1H), 2.76–2.68 (m, 1H), 2.19–2.08 (m, 2H), 1.95–1.64 (m, 7H), 1.59–1.39 (m, 6H).

^{13}C NMR (126 MHz, DMSO-d_6): δ 171.3, 166.0, 165.4, 160.5, 158.6, 158.1, 153.8, 136.0, 132.3, 128.9, 128.6, 128.3, 127.8, 126.3, 124.5, 124.3, 123.7, 114.9, 112.1, 56.4, 55.5, 42.9, 34.2, 33.3, 33.0, 30.3, 28.5, 28.5, 25.0, 24.9, 23.0, 22.4.

LC-MS (ESI): t_R = 4.75 min, area: 97%, *m/z* 547 $[M+H]^+$.

HRMS (ESI) *m/z*: $[M+H]^+$ calcd. for $C_{31}H_{36}N_4O_4F$ 547.2715, found 547.2702.

*4.6.2.10. N-(2-Amino-2-oxoethyl)-5′-(cis-3-cycloheptyl-4-oxo-3,4,4a,5,8,8a-hexahydrophthalazin-1-yl)-2′-methoxy-2-methyl-[1,1′-biphenyl]-4-carboxamide (**4b**).* To a solution of glycinamide.HCl (34.1 mg, 0.31 mmol) and **10c** (75 mg, 0.15 mmol) in DCM (3 mL) was added DIPEA (0.34 mmol, 60 µL), EDC.HCl (65 mg, 0.34 mmol) and HOAt (42 mg, 0.31 mmol). The mixture was stirred at rt for 1 h. The reaction mixture was diluted with water (10 mL) and extracted with EtOAc (3 × 25 mL). The combined organic phases were washed with water (15 mL), brine (15 mL), dried over Na_2SO_4, filtered and concentrated. The residue was purified on a reverse phase silica gel column eluting with MeCN/H_2O + 0.1% formic acid (gradient, 5–95%) to afford **4b** as a light yellow solid (71 mg, 83%).

^{1}H NMR (500 MHz, DMSO-d_6): δ 8.69 (t, J = 5.9 Hz, 1H), 7.90 (dd, J = 8.8, 2.2 Hz, 1H), 7.81 (s, 1H), 7.74 (dd, J = 7.8, 1.7 Hz, 1H), 7.60 (d, J = 2.1 Hz, 1H), 7.41 (s, 1H), 7.25 (d, J = 7.8 Hz, 1H), 7.21 (d, J = 8.7 Hz, 1H), 7.09 (s, 1H), 5.73–5.58 (m, 2H), 4.68 (tt, J = 9.6, 5.0 Hz, 1H), 3.83 (d, J = 5.8 Hz, 2H), 3.78 (s, 3H), 3.46 (dt, J = 11.6, 5.7 Hz, 1H), 2.80 (t, J = 6.1 Hz, 1H), 2.77–2.68 (m, 1H), 2.13 (s, 5H), 1.93–1.65 (m, 7H), 1.61–1.40 (m, 6H).

^{13}C NMR (126 MHz, DMSO-d_6): δ 171.5, 166.8, 166.0, 157.8, 154.0, 141.4, 136.7, 133.7, 130.3, 130.0, 129.0, 128.1, 127.6, 127.6, 126.4, 125.1, 124.5, 111.9, 56.1, 55.5, 42.9, 34.2, 33.3, 33.1, 30.3, 28.5, 28.5, 25.0, 24.9, 23.0, 22.4, 20.1.

LC-MS (ESI): t_R = 4.80 min, area: > 98%, *m/z* 543 $[M+H]^+$.

HRMS (ESI) *m/z*: $[M+H]^+$ calcd. for $C_{32}H_{39}N_4O_4$ 543.2966, found 543.2949.

*4.6.2.11. N-(2-Amino-2-oxoethyl)-5′-(cis-3-cycloheptyl-4-oxo-3,4,4a,5,8,8a-hexahydrophthalazin-1-yl)-2,2′-dimethoxy-[1,1′-biphenyl]-4-carboxamide (**4c**).* This compound was prepared from **11** (100 mg, 0.21 mmol) and **12b** (60 mg, 0.21 mmol) as described for **4a**. The title compound was obtained as a light yellow solid (62 mg, 52%).

^{1}H NMR (500 MHz, DMSO-d_6): δ 8.75 (t, J = 6.0 Hz, 1H), 7.83 (dd, J = 8.7, 2.1 Hz, 1H), 7.64 (d, J = 2.3 Hz, 1H), 7.56 (s, 1H), 7.52 (d, J = 7.8 Hz, 1H), 7.40 (s, 1H), 7.27 (d, J = 7.7 Hz, 1H), 7.15 (d, J = 8.7 Hz, 1H), 7.08 (s, 1H), 5.72–5.58 (m, 2H), 4.71–4.62 (m, 1H), 3.84 (d, J = 5.8 Hz, 2H), 3.77 (s, 3H), 3.75 (s, 3H), 3.43 (dt, J = 11.7, 5.8 Hz, 1H), 2.81–2.68 (m, 2H), 2.20–2.07 (m, 2H), 1.94–1.64 (m, 7H), 1.61–1.37 (m, 6H).

^{13}C NMR (126 MHz, DMSO-d_6): δ 171.5, 166.6, 166.0, 158.4, 157.0, 154.0, 135.2, 131.3, 130.4, 128.6, 127.4, 127.4, 127.3, 126.4, 124.5, 119.8, 111.9, 110.6, 56.2, 56.1, 55.4, 42.9, 34.2, 33.3, 33.0, 30.4, 28.6, 28.5, 24.9, 24.9, 23.1, 22.4.

LC-MS (ESI): t_R = 4.65 min, area: 95%, *m/z* 559 $[M+H]^+$.

HRMS (ESI) *m/z*: $[M+H]^+$ calcd. for $C_{32}H_{39}N_4O_5$ 559.2915, found 559.2913.

*4.6.2.12. N-(2-Amino-2-oxoethyl)-5′-(cis-3-cycloheptyl-4-oxo-3,4,4a,5,8,8a-hexahydrophthalazin-1-yl)-3-fluoro-2′-methoxy-[1,1′-biphenyl]-4-carboxamide (**4d**).* This compound was prepared from **10a**

(150 mg, 0.31 mmol) and glycinamide.HCl (68 mg, 0.61 mmol) as described for **4b**. The title compound was obtained as a light yellow solid (40 mg, 23%).

^{1}H NMR (500 MHz, DMSO-d_6): δ 8.43–8.34 (m, 1H), 7.92 (dd, J = 8.8, 2.3 Hz, 1H), 7.84–7.76 (m, 2H), 7.51–7.40 (m, 3H), 7.26 (d, J = 8.8 Hz, 1H), 7.19–7.12 (m, 1H), 5.75–5.58 (m, 2H), 4.69 (tt, J = 9.0, 4.4 Hz, 1H), 3.86 (d, J = 8.3 Hz, 5H), 3.53 (dt, J = 11.6, 5.7 Hz, 1H), 2.82–2.69 (m, 2H), 2.21–2.09 (m, 2H), 1.97–1.88 (m, 1H), 1.87–1.67 (m, 6H), 1.62–1.41 (m, 6H).

^{13}C NMR (126 MHz, DMSO-d_6): δ 170.9, 166.0, 163.7, 160.6, 158.6, 157.7, 153.9, 142.8, 130.7, 128.3, 128.1, 126.3, 125.8, 124.5, 121.8, 117.4, 112.7, 56.4, 55.4, 42.9, 34.2, 33.3, 33.1, 30.2, 28.7, 28.6, 25.0, 24.9, 23.0, 22.4.

LC-MS (ESI): t_R = 4.87 min, area: > 98%, m/z 547 $[M+H]^+$.

HRMS (ESI) m/z: $[M+H]^+$ calcd. for $C_{31}H_{36}N_4O_4F$ 547.2707, found 547.2715.

*4.6.2.13. N-(2-Amino-2-oxoethyl)-5′-(cis-3-cycloheptyl-4-oxo-3,4,4a,5,8,8a-hexahydrophthalazin-1-yl)-2′-methoxy-3-methyl-[1,1′-biphenyl]-4-carboxamide (**4e**)*. This compound was prepared from **11** (200 mg, 0.42 mmol) and **12c** (113 mg, 0.42 mmol) as described for **4a**. The title compound was obtained as a light yellow solid (130 mg, 57%).

^{1}H NMR (500 MHz, DMSO-d_6): δ 8.39 (t, J = 6.0 Hz, 1H), 7.85 (dd, J = 8.7, 2.2 Hz, 1H), 7.74 (d, J = 2.1 Hz, 1H), 7.48 (d, J = 7.8 Hz, 1H), 7.40–7.30 (m, 3H), 7.20 (d, J = 8.7 Hz, 1H), 7.06 (s, 1H), 5.73–5.57 (m, 2H), 4.73–4.64 (m, 1H), 3.85–3.75 (m, 5H), 3.52–3.43 (m, 1H), 2.82–2.69 (m, 2H), 2.40 (s, 3H), 2.20–2.07 (m, 2H), 1.95–1.65 (m, 7H), 1.62–1.38 (m, 6H).

^{13}C NMR (126 MHz, DMSO-d_6): δ 171.3, 169.6, 166.0, 157.8, 154.0, 139.3, 135.9, 135.7, 131.7, 130.0, 128.1, 127.8, 127.6, 127.4, 126.8, 126.4, 124.5, 112.3, 56.3, 55.3, 42.6, 34.2, 33.3, 33.0, 30.3, 28.7, 28.7, 24.9, 24.8, 23.0, 22.4, 20.1.

LC-MS (ESI): t_R = 4.83 min, area: 98%, m/z 543 $[M+H]^+$.

HRMS (ESI) m/z: $[M+H]^+$ calcd. for $C_{32}H_{39}N_4O_4$ 543.2950, found 543.2966.

*4.6.2.14. N-(2-Amino-2-oxoethyl)-5′-(cis-3-cycloheptyl-4-oxo-3,4,4a,5,8,8a-hexahydrophthalazin-1-yl)-2′,3-dimethoxy-[1,1′-biphenyl]-4-carboxamide (**4f**)*. This compound was prepared from **11** (200 mg, 0.42 mmol) and **12d** (120 mg, 0.42 mmol) as described for **4a**. The title compound was obtained as a light yellow solid (137 mg, 58%).

^{1}H NMR (500 MHz, DMSO-d_6): δ 8.57 (t, J = 5.3 Hz, 1H), 7.93 (d, J = 8.0 Hz, 1H), 7.89 (dd, J = 8.7, 2.2 Hz, 1H), 7.83 (d, J = 2.1 Hz, 1H), 7.42 (s, 1H), 7.28–7.18 (m, 3H), 7.14 (s, 1H), 5.74–5.59 (m, 2H), 4.70 (tt, J = 8.5, 4.9 Hz, 1H), 3.97 (s, 3H), 3.92 (d, J = 5.2 Hz, 2H), 3.85 (s, 3H), 3.50 (dt, J = 11.5, 5.7 Hz, 1H), 2.83–2.71 (m, 2H), 2.22–2.09 (m, 2H), 1.97–1.68 (m, 7H), 1.62–1.41 (m, 6H).

^{13}C NMR (126 MHz, DMSO-d_6): δ 171.1, 166.0, 164.7, 157.8, 157.4, 153.9, 142.7, 131.0, 129.6, 128.2, 127.9, 127.7, 126.4, 124.5, 122.2, 120.9, 113.6, 112.5, 56.5, 56.4, 55.4, 43.1, 34.3, 33.3, 33.1, 30.3, 28.8, 28.7, 24.9, 24.8, 23.0, 22.4.

LC-MS (ESI): t_R = 4.86 min, area: 97%, m/z 559 $[M+H]^+$.

HRMS (ESI) m/z: $[M+H]^+$ calcd. for $C_{32}H_{39}N_4O_5$ 559.2915, found 559.2887.

*4.6.2.15. cis-2-Cycloheptyl-4-(4-methoxy-3-(1-oxoisoindolin-5-yl)phenyl)-4a,5,8,8a-tetrahydrophthalazin-1(2H)-one (**5a**)*. To an argon purged solution of **9** (1.4 g, 3.1 mmol) in DME (15 mL) was added 5-(4,4,5,5-tetramethyl-1,3,2-dioxaborolan-2-yl)isoindolin-1-one (0.84 g, 3.2 mmol), $PdCl_2$(dppf) (0.11 g, 0.15 mmol) and aq. Na_2CO_3 (2 M, 9.3 mmol, 4.6 mL). The reaction mixture was stirred at 100 °C for 5 h. The reaction mixture was diluted with DCM (250 mL) and washed with sat. aq. NH_4Cl (150 mL), water (150 mL) and brine (200 mL). The organic phase was dried over Na_2SO_4, filtered and concentrated. The residue was purified on a reverse phase silica gel column eluting with MeCN/H_2O + 0.1% formic acid (gradient, 5–95%) to afford **5a** as a light brown solid (1.2 g, 73%).

^{1}H NMR (500 MHz, DMSO-d_6): δ 8.61 (s, 1H), 7.92 (dd, J = 8.7, 2.2 Hz, 1H), 7.76 (d, J = 2.2 Hz, 1H), 7.72 (d, J = 7.9 Hz, 1H), 7.68 (s, 1H), 7.59 (d, J = 7.8 Hz, 1H), 7.26 (d, J = 8.8 Hz, 1H), 5.75–5.59 (m, 2H), 4.69 (tt, J = 10.0, 4.7 Hz, 1H), 4.43 (s, 2H), 3.83 (s, 3H), 3.50 (dt, J = 11.5, 5.7 Hz, 1H), 3.34 (s, 1H), 2.80 (t, J = 6.1 Hz, 1H), 2.77–2.69 (m, 1H), 2.21–2.09 (m, 2H), 1.96–1.67 (m, 6H), 1.62–1.40 (m, 6H).

^{13}C NMR (126 MHz, DMSO-d_6): δ 170.2, 166.0, 157.7, 154.0, 144.5, 141.4, 131.9, 129.9, 129.5, 128.5, 128.0, 127.6, 126.4, 125.0, 124.5, 122.8, 112.6, 56.4, 55.4, 45.4, 34.2, 33.3, 33.1, 30.3, 28.6, 28.6, 25.0, 24.9, 23.0, 22.4.

LC-MS (ESI): t_R = 5.05 min, area: > 98%, m/z 484 $[M+H]^+$.

HRMS (ESI) m/z: $[M+H]^+$ calcd. for $C_{30}H_{34}N_3O_3$ 484.2595, found 484.2585.

*4.6.2.16. cis-2-Cycloheptyl-4-(4-methoxy-3-(2-(2-methoxyethyl)-1-oxoisoindolin-5-yl)phenyl)-4a,5,8,8a-tetrahydrophthalazin-1(2H)-one (**5b**)*. To an ice-cooled solution of **5a** (0.10 g, 0.19 mmol) in DMF (1.5 mL) was added NaH (23 mg, 0.57 mmol, 60%). The mixture was stirred for 0.5 h at rt prior to the addition of 1-bromo-2-methoxyethane (40 µL, 0.41 mmol). The reaction mixture was stirred at rt for 1.5 h. The reaction mixture was quenched with water (20 mL) and extracted with DCM (2 × 30 mL). The combined organic phases were washed with brine (25 mL), dried over Na_2SO_4, filtered and concentrated. The residue was purified on a silica gel column eluting with EtOAc/*n*-heptane (gradient, 25–66%) to afford **5b** as a white solid (31 mg, 27%).

^{1}H NMR (500 MHz, DMSO-d_6): δ 7.91 (dt, J = 8.8, 1.8 Hz, 1H), 7.76 (t, J = 1.9 Hz, 1H), 7.75–7.68 (m, 2H), 7.60 (d, J = 7.8 Hz, 1H), 7.25 (dd, J = 8.8, 1.2 Hz, 1H), 5.74–5.59 (m, 2H), 4.73–4.65 (m, 1H), 4.57 (s, 2H), 3.84 (d, J = 1.3 Hz, 3H), 3.72 (t, J = 5.4 Hz, 2H), 3.59 (t, J = 5.4 Hz, 2H), 3.50 (dt, J = 11.6, 5.8 Hz, 1H), 3.29 (s, 3H), 2.83–2.71 (m, 2H), 2.22–2.09 (m, 2H), 1.97–1.67 (m, 7H), 1.61–1.42 (m, 6H).

^{13}C NMR (126 MHz, DMSO-d_6): δ 167.5, 166.0, 157.7, 154.0, 142.4, 141.3, 131.6, 129.9, 129.6, 128.5, 128.0, 127.6, 126.4, 124.7, 124.5, 122.7, 112.6, 70.6, 58.4, 56.4, 55.5, 50.8, 41.8, 34.3, 33.3, 33.1, 30.4, 28.6, 28.6, 25.0, 24.9, 23.0, 22.4.

LC-MS (ESI): t_R = 5.39 min, area: 95%, m/z 542 $[M+H]^+$.

HRMS (ESI) m/z: $[M+H]^+$ calcd. for $C_{33}H_{40}N_3O_4$ 542.3013, found 542.3000.

*4.6.2.17. 2-(5-(5-(cis-3-Cycloheptyl-4-oxo-3,4,4a,5,8,8a-hexahydrophthalazin-1-yl)-2-methoxyphenyl)-1-oxoisoindolin-2-yl) acetamide (**5c**)*. This compound was prepared from **5a** (0.10 mg, 0.21 mmol) and 2-bromoacetamide (31 mg, 0.23 mmol) as described for **5b**. The title compound was obtained as a white solid (29 mg, 26%).

^{1}H NMR (500 MHz, DMSO-d_6): δ 7.91 (dd, J = 8.7, 2.2 Hz, 1H), 7.78 (d, J = 2.3 Hz, 1H), 7.75 (d, J = 7.9 Hz, 1H), 7.71 (s, 1H), 7.61 (d, J = 7.8 Hz, 1H), 7.57 (s, 1H), 7.26 (d, J = 8.7 Hz, 1H), 7.17 (s, 1H), 5.74–5.59 (m, 2H), 4.69 (tt, J = 8.8, 4.9 Hz, 1H), 4.57 (s, 2H), 4.16 (s, 2H), 3.84 (s, 3H), 3.50 (dt, J = 11.5, 5.7 Hz, 1H), 2.83–2.70 (m, 2H), 2.22–2.10 (m, 2H), 1.97–1.67 (m, 7H), 1.61–1.41 (m, 6H).

^{13}C NMR (126 MHz, DMSO-d_6): δ 170.4, 168.0, 166.0, 157.8, 154.0, 142.7, 141.5, 131.3, 130.0, 129.6, 128.5, 128.0, 127.7, 126.4, 124.7, 124.5, 122.9, 112.6, 56.4, 55.5, 51.0, 45.0, 34.3, 33.3, 33.1, 30.4, 28.6, 28.6, 25.0, 24.9, 23.0, 22.4.

LC-MS (ESI): t_R = 4.75 min, area: > 98%, m/z 541 $[M+H]^+$.

HRMS (ESI) m/z: $[M+H]^+$ calcd. for $C_{32}H_{37}N_4O_4$ 541.2809, found 541.2788.

*4.6.2.18. N-(2-Amino-2-oxoethyl)-3-(5-(cis-3-cycloheptyl-4-oxo-3,4,4a,5,8,8a-hexahydrophthalazin-1-yl)-2-methoxyphenyl)propiolamide (**8g**)*. A N_2-flushed mixture of **9** (1.0 g, 2.32 mmol), $Pd(PPh_3)_2Cl_2$ (49.0 mg, 0.07 mmol), propiolic acid (0.16 mL, 2.55 mmol), DBU (1.73 mL, 11.59 mmol) and dppb (79.0 mg, 0.19 mmol) in DMSO (6 mL) was stirred at 50 °C for 15 h. The reaction mixture was diluted with EtOAc (300 mL) and washed with sat. aq. $NaHCO_3$ (150 mL). The aqueous phase was acidified using sat. aq. NH_4Cl (~250 mL) and

extracted with EtOAc (2 × 400 mL). The combined organic phases were dried over Na_2SO_4, filtered and concentrated to obtain the crude material of carboxylic acid **13** (320 mg). A portion of the residue (100 mg) was dissolved in DMF (3 mL) and glycinamide.HCl (52 mg, 0.48 mmol), DIPEA (0.10 mL, 0.60 mmol), EDC (50 mg, 0.26 mmol) and HOAt (32 mg, 0.24 mmol) were added. This mixture was stirred at rt for 30 h. The reaction mixture was diluted with water (25 mL) and extracted with EtOAc (3 × 75 mL). The combined organic phases were combined and washed with water (4 × 25 mL) and brine (3 × 25 mL). The organic phase was dried over Na_2SO_4 and concentrated. The residue was purified on a silica gel column eluting with MeOH/DCM (gradient, 0–1.5%) to afford **8g** as a white solid (6 mg). The extrapolated yield of this reaction is 1.5%.

^{1}H NMR (500 MHz, DMSO-d_6): δ 8.91 (t, J = 6.1 Hz, 1H), 7.98 (dd, J = 8.9, 2.3 Hz, 1H), 7.95 (d, J = 2.3 Hz, 1H), 7.43 (s, 1H), 7.23 (d, J = 8.9 Hz, 1H), 7.09 (s, 1H), 5.74–5.58 (m, 2H), 4.67 (tt, J = 9.0, 4.4 Hz, 1H), 3.92 (s, 3H), 3.72 (d, J = 6.0 Hz, 2H), 3.45 (dt, J = 11.7, 5.8 Hz, 1H), 2.81 (t, J = 6.1 Hz, 1H), 2.74 (app. d, 1H), 2.14 (app. t, 2H), 1.98–1.89 (m, 1H), 1.83–1.67 (m, 6H), 1.61–1.43 (m, 7H).

^{13}C NMR (126 MHz, DMSO-d_6): δ 170.5, 166.1, 161.8, 153.1, 153.1, 131.6, 130.0, 127.9, 126.4, 124.4, 112.4, 109.5, 88.2, 80.7, 56.6, 55.7, 42.3, 34.1, 33.3, 33.1, 30.3, 28.4, 28.3, 25.0, 24.9, 22.9, 22.4.

LC-MS (ESI): t_R = 4.44 min, area: > 98%, m/z 477 $[M+H]^+$.

HRMS (ESI) m/z: $[M+H]^+$ calcd. for $C_{27}H_{33}N_4O_4$ 477.2496, found 477.2480.

*4.6.2.19. Methyl-3-(5-(cis-3-cycloheptyl-4-oxo-3,4,4a,5,8,8a-hexahydrophthalazin-1-yl)-2-methoxyphenyl)propiolate **(14)***. To a solution of **11** (900 mg, 1.88 mmol) in anhydrous acetonitrile (15 mL) was added Pd(II)$(OAc)_2$ (21 mg, 94 μmol), K_2CO_3 (520 mg, 3.76 mmol), Ag(II)O (654 mg, 2.82 mmol) and methyl propiolate (174 mg, 2.07 mmol, 0.18 mL). The mixture was heated to 70 °C for 2.5 h. The reaction mixture was filtered over Hyflo. The filtrate was diluted with EtOAc (15 mL) and washed with water (2 × 10 mL) and brine (10 mL). The organic phase was dried over Na_2SO_4, filtered and concentrated. The residue was purified on a silica gel column eluting with EtOAc/*n*-heptane (gradient, 10–20%) to afford **14** as a white solid (489 mg, 53%).

^{1}H-NMR (300 MHz, DMSO-d_6): δ 8.05 (dd, J = 2.3 Hz, J = 8.8 Hz, 1H), 8.01 (d, J = 2.3 Hz, 1H), 7.26 (d, J = 8.8 Hz, 1H), 5.81–5.53 (m, 2H), 4.13–4.01 (m, 1H), 3.93 (s, 3H), 3.78 (s, 3H), 3.48 (q, J = 5.6 Hz, 1H), 2.82–2.68 (m, 2H), 2.21–2.05 (m, 2H), 1.98–1.36 (m, 13H).

LC-MS (ESI): t_R = 3.95 min, area: > 95%, m/z 435 $[M+H]^+$.

*4.6.2.20. 3-(5-(cis-3-Cycloheptyl-4-oxo-3,4,4a,5,8,8a-hexahydrophthalazin-1-yl)-2-methoxyphenyl)propiolamide **(8b)***. Compound **14** (60 mg, 0.12 mmol) was dissolved in a solution of NH_3 in MeOH (7 M, 2 mL). This mixture was stirred at rt for 2 h. The solvent was evaporated to obtain **8b** as a white solid (52 mg, 89%).

^{1}H NMR (500 MHz, $CDCl_3$): δ 7.99–7.84 (m, 2H), 7.02–6.90 (m, 1H), 6.35 (s, 1H), 6.14 (s, 1H), 5.85–5.59 (m, 2H), 4.88–4.72 (m, 1H), 3.94 (s, 3H), 3.25 (dt, J = 11.5, 5.7 Hz, 1H), 3.05–2.92 (m, 1H), 2.72 (t, J = 6.0 Hz, 1H), 2.26–2.08 (m, 2H), 2.05–1.95 (m, 2H), 1.92–1.84 (m, 1H), 1.82–1.69 (m, 4H), 1.69–1.43 (m, 6H), 1.34–1.20 (m, 2H).

^{13}C NMR (126 MHz, $CDCl_3$): δ 165.9, 161.9, 155.2, 152.3, 132.0, 129.5, 127.9, 126.0, 123.8, 111.0, 109.5, 86.5, 82.3, 56.4, 56.1, 34.6, 33.2, 33.0, 30.9, 28.2, 28.1, 25.1, 25.0, 22.9, 22.3.

LC-MS (ESI): t_R = 4.82 min, area: > 98%, m/z 420 $[M+H]^+$.

HRMS (ESI) m/z: $[M+H]^+$ calcd. for $C_{25}H_{30}N_3O_3$ 420.2282, found 420.2278.

*4.6.2.21. N-Butyl-3-(5-(cis-3-cycloheptyl-4-oxo-3,4,4a,5,8,8a-hexahydrophthalazin-1-yl)-2-methoxyphenyl)propiolamide **(8c)***. To an ice-cooled solution of **14** (60 mg, 0.12 mmol) and butan-1-amine (15 μL, 0.15 mmol) in toluene (2 mL) was slowly added $AlMe_3$ in toluene (2 M, 93 μL, 0.19 mmol,). The reaction mixture was stirred at 50 °C for 1 day. The reaction mixture was diluted with water (10 mL) and extracted with EtOAc (3 × 15 mL). The combined organic phases were washed with brine (25 mL), dried over Na_2SO_4, filtered and concentrated. The residue was purified on a silica gel column eluting with MeOH/DCM (gradient, 0–1.5%) to afford **8c** as a white solid (10 mg, 17%).

^{1}H NMR (500 MHz, DMSO-d_6): δ 8.75 (t, J = 5.8 Hz, 1H), 7.95 (dd, J = 8.9, 2.3 Hz, 1H), 7.90 (d, J = 2.3 Hz, 1H), 7.21 (d, J = 9.0 Hz, 1H), 5.73–5.57 (m, 2H), 4.65 (tt, J = 9.7, 4.5 Hz, 1H), 3.90 (s, 3H), 3.47–3.39 (m, 1H), 3.16–3.07 (m, 2H), 2.78 (t, J = 6.1 Hz, 1H), 2.76–2.67 (m, 1H), 2.20–2.03 (m, 2H), 1.96–1.85 (m, 1H), 1.85–1.18 (m, 16H), 0.87 (t, J = 7.3 Hz, 3H).

^{13}C NMR (126 MHz, DMSO-d_6): δ 166.0, 161.7, 153.1, 152.6, 131.5, 129.8, 127.8, 126.3, 124.4, 112.4, 109.6, 88.4, 79.9, 56.5, 55.6, 39.1, 34.1, 33.3, 33.1, 31.3, 30.3, 28.4, 28.3, 25.0, 24.9, 22.8, 22.4, 20.0, 14.1.

LC-MS (ESI): t_R = 5.56 min, area: > 98%, m/z 476 $[M+H]^+$.

HRMS (ESI) m/z: $[M+H]^+$ calcd. for $C_{29}H_{38}N_3O_3$ 476.2908, found 476.2887.

*4.6.2.22. 3-(5-(cis-3-Cycloheptyl-4-oxo-3,4,4a,5,8,8a-hexahydrophthalazin-1-yl)-2-methoxyphenyl)-N-(2-methoxyethyl) propiolamide **(8d)***. This compound was prepared from **14** (60 mg, 0.12 mmol) and 2-methoxyethanamine (13 μL, 0.15 mmol) as described for **8c**. The title compound was obtained as a white solid (11 mg, 19%).

^{1}H NMR (500 MHz, DMSO-d_6): δ 8.83 (t, J = 5.7 Hz, 1H), 8.02–7.89 (m, 2H), 7.21 (d, J = 8.9 Hz, 1H), 5.75–5.56 (m, 2H), 4.66 (tt, J = 9.5, 4.8 Hz, 1H), 3.90 (s, 3H), 3.47–3.37 (m, 3H), 3.33–3.26 (m, 2H), 3.25 (s, 3H), 2.84–2.67 (m, 2H), 2.19–2.05 (m, 2H), 1.97–1.86 (m, 1H), 1.84–1.37 (m, 13H).

^{13}C NMR (126 MHz, DMSO-d_6): δ 166.0, 161.8, 153.1, 152.9, 131.5, 129.9, 127.8, 126.3, 124.4, 112.4, 109.6, 88.3, 80.2, 70.5, 58.3, 56.6, 55.6, 39.2, 34.1, 33.3, 33.1, 30.3, 28.4, 28.3, 25.0, 24.9, 22.8, 22.4.

LC-MS (ESI): t_R = 5.12 min, area: > 98%, m/z 478 $[M+H]^+$.

HRMS (ESI) m/z: $[M+H]^+$ calcd. for $C_{28}H_{36}N_3O_4$ 478.2700, found 478.2678.

*4.6.2.23. cis-2-Cycloheptyl-4-(4-methoxy-3-(3-morpholino-3-oxoprop-1-yn-1-yl)phenyl)-4a,5,8,8a-tetrahydrophthalazin-1(2H)-one **(8e)***. This compound was prepared from **14** (60 mg, 0.12 mmol) and morpholine (11 μL, 0.12 mmol) as described for **8c**. The title compound was obtained as a white solid (22 mg, 37%).

^{1}H NMR (500 MHz, DMSO-d_6): δ 8.03–7.96 (m, 2H), 7.24 (d, J = 8.7 Hz, 1H), 5.74–5.57 (m, 2H), 4.65 (m, J = 9.3, 4.3 Hz, 1H), 3.92 (s, 3H), 3.83 (t, J = 4.8 Hz, 2H), 3.69 (t, J = 4.8 Hz, 2H), 3.64–3.53 (m, 4H), 3.48 (dt, J = 11.6, 5.8 Hz, 1H), 2.79 (t, J = 6.1 Hz, 1H), 2.77–2.69 (m, 1H), 2.21–2.05 (m, 2H), 1.98–1.87 (m, 1H), 1.85–1.65 (m, 6H), 1.63–1.39 (m, 6H).

^{13}C NMR (126 MHz, DMSO-d_6): δ 166.1, 162.1, 153.1, 152.4, 131.5, 130.4, 128.0, 126.3, 124.5, 112.4, 109.2, 86.7, 85.7, 66.7, 66.2, 56.8, 55.5, 47.2, 42.0, 34.2, 33.3, 33.1, 30.1, 28.5, 28.5, 25.0, 24.9, 22.8, 22.4.

LC-MS (ESI): t_R = 5.23 min, area: > 98%, m/z 490 $[M+H]^+$.

HRMS (ESI) m/z: $[M+H]^+$ calcd. for $C_{29}H_{36}N_3O_4$ 490.2700, found 490.2684.

*4.6.2.24. 3-(5-(cis-3-Cycloheptyl-4-oxo-3,4,4a,5,8,8a-hexahydrophthalazin-1-yl)-2-methoxyphenyl)-N-(furan-2-ylmethyl) propiolamide **(8f)***. This compound was prepared from **14** (60 mg, 0.12 mmol) and furan-2-ylmethanamine (13 μL, 0.15 mmol) as described for **8c**. The title compound was obtained as a white solid (10 mg, 16%).

^{1}H NMR (500 MHz, $CDCl_3$): δ 8.01–7.83 (m, 2H), 7.39 (s, 1H), 6.95 (d, J = 8.6 Hz, 1H), 6.42 (t, J = 5.7 Hz, 1H), 6.38–6.28 (m, 2H), 5.84–5.62 (m, 2H), 4.85–4.74 (m, 1H), 4.55 (d, J = 5.6 Hz, 2H), 3.93

(s, 3H), 3.24 (dt, J = 11.5, 5.7 Hz, 1H), 3.07–2.94 (m, 1H), 2.71 (t, J = 6.1 Hz, 1H), 2.27–2.09 (m, 2H), 2.05–1.93 (m, 2H), 1.93–1.83 (m, 1H), 1.83–1.69 (m, 4H), 1.69–1.43 (m, 6H),

^{13}C NMR (126 MHz, $CDCl_3$): δ 165.9, 161.8, 153.1, 152.3, 150.3, 142.4, 132.0, 129.3, 127.9, 126.0, 123.7, 111.0, 110.6, 109.6, 108.1, 86.8, 81.6, 56.4, 56.1, 36.7, 34.6, 33.2, 33.0, 30.9, 28.2, 28.1, 25.1, 25.0, 22.9, 22.3.

LC-MS (ESI): t_R = 5.35 min, area: > 98%, m/z 500 $[M+H]^+$.

HRMS (ESI) m/z: $[M+H]^+$ calcd. for $C_{30}H_{34}N_3O_4$ 500.2544, found 500.2539.

4.6.2.25. cis-2-Cycloheptyl-4-(4-methoxy-3-((trimethylsilyl)ethynyl) phenyl)-4a,5,8,8a-tetrahydrophthalazin-1(2H)-one ***(15)***. To an argon purged solution of $Pd(PPh_3)_2Cl_2$ (15 mg, 21 mmol) and **9** (0.10 g, 0.21 mmol) in Et_3N (2.0 mL, 14 mmol) was added ethynyltrimethylsilane (60 µL, 0.43 mmol) and CuI (4.0 mg, 0.02 mmol). The reaction mixture was stirred at 80 °C for 3 h. The reaction mixture was filtered over Celite and partitioned between EtOAc (40 mL) and sat. aq. NH_4Cl/H_2O (1:2, 30 mL). The organic phase was washed with water (30 mL) and brine (30 mL), dried over Na_2SO_4, filtered and concentrated. The residue was purified on a silica gel column eluting with EtOAc/*n*-heptane (gradient, 5–25%) to afford **15** as a white solid (77 mg, 80%).

^{1}H NMR (400 MHz, DMSO-d_6): δ 7.87 (dd, J = 8.8, 1.8 Hz, 1H), 7.79 (d, J = 1.8 Hz, 1H), 7.15 (d, J = 8.9 Hz, 1H), 5.76–5.56 (m, 2H), 4.77–4.57 (m, 1H), 3.86 (s, 3H), 3.48–3.40 (m, 1H), 2.84–2.63 (m, 2H), 2.27–1.13 (m, 15H), 0.23 (s, 9H).

LC-MS (ESI): t_R = 2.74 min, area: > 97%, m/z 449 $[M+H]^+$.

4.6.2.26. cis-2-Cycloheptyl-4-(3-ethynyl-4-methoxyphenyl)-4a,5,8,8a-tetrahydrophthalazin-1(2H)-one ***(8a)***. To a suspension of **15** (1.2 g, 3.04 mmol) in MeOH (15 mL) was added NaOH (1.0 M, 6 mL). The mixture was stirred at rt for 2 h. The reaction mixture was diluted with EtOAc (100 mL) and washed with water (2 × 50 mL) and brine (50 mL). The organic phase was dried over $MgSO_4$, filtered and concentrated to obtain **8a** (890 mg, 91%) as a light yellow solid.

^{1}H NMR (500 MHz, DMSO-d_6): δ 7.91–7.85 (m, 2H), 7.19–7.12 (m, 1H), 5.74–5.59 (m, 2H), 4.68 (tt, J = 9.2, 4.6 Hz, 1H), 4.31 (s, 1H), 3.88 (s, 3H), 3.44 (dt, J = 11.5, 5.7 Hz, 1H), 2.82–2.70 (m, 2H), 2.22–2.05 (m, 2H), 1.97–1.87 (m, 1H), 1.85–1.66 (m, 6H), 1.63–1.41 (m, 6H).

^{13}C NMR (126 MHz, DMSO-d_6): δ 166.0, 161.6, 153.3, 131.2, 128.7, 127.7, 126.3, 124.4, 112.0, 111.5, 85.4, 80.2, 56.4, 55.6, 34.2, 33.3, 33.1, 30.3, 28.5, 28.5, 25.0, 24.9, 22.9, 22.4.

LC-MS (ESI): t_R = 5.60 min, area: 95%, m/z 377 $[M+H]^+$.

HRMS (ESI) m/z: $[M+H]^+$ calcd. for $C_{24}H_{29}N_2O_2$ 377.2224, found 377.2213.

4.6.2.27. 3-(5-(cis-3-Cycloheptyl-4-oxo-3,4,4a,5,8,8a-hexahydrophthalazin-1-yl)-2-methoxyphenyl)propiolaldehyde ***(16)***. Compound **8a** (100 mg, 0.266 mmol) was dissolved in THF (2 mL) and the mixture was cooled to −78 °C. To this mixture was added 1.6 M *n*-BuLi in hexane (0.20 mL, 0.32 mmol,) and the mixture was stirred for 30 min prior to the addition of DMF (0.031 mL, 0.40 mmol). After 1.5 h, the reaction mixture was poured into acidified ice water (50 mL) and was neutralized to pH 6–7. The product was extracted with EtOAc (3 × 50 mL). The combined organic phases were washed with brine (100 mL), dried over Na_2SO_4, filtered and concentrated. The product was purified with flash column chromatography (5–40% EtOAc/Hept) and to give **16** as a white solid (74 mg, 69%).

^{1}H NMR (300 MHz, DMSO-d_6): δ 9.45 (s, 1H), 8.07–8.03 (m, 2H), 7.27 (d, J = 8.9 Hz, 1H), 5.71–5.60 (m, 2H), 4.65 (hept, J = 4.5 Hz, 1H), 3.94 (s, 3H), 3.47 (dt, J = 11.4, 5.8 Hz, 1H), 2.80–2.67 (m, 2H), 2.15–2.04 (m, 2H), 1.96–1.43 (m, 13H)

4.6.2.28. cis-2-Cycloheptyl-4-(4-methoxy-3-(oxazol-5-ylethynyl)phenyl)-4a,5,8,8a-tetrahydrophthalazin-1(2H)-one ***(8h)***. To a solution of **16** (74 mg, 0.18 mmol) in MeOH (3 mL) was added 1-((isocyanomethyl) sulfonyl)-4-methylbenzene (38 mg, 0.19 mmol) and K_2CO_3 (28 mg, 0.20 mmol). This mixture was heated to reflux for 1.5 h. The mixture was diluted with EtOAc (25 mL) and washed with sat. aq. NH_4Cl (25 mL), water (25 mL) and brine (25 mL). The organic phase was dried over Na_2SO_4, filtered and concentrated to gain a brown oil. The product was purified with reverse phase column purification to obtain the product as a white solid after lyophilisation (38 mg, 47%).

^{1}H NMR (500 MHz, DMSO-d_6): δ 8.54 (s, 1H), 7.96 (s, 2H), 7.67 (s, 1H), 7.24 (d, J = 8.6 Hz, 1H), 5.75–5.58 (m, 2H), 4.68 (tt, J = 9.3, 4.5 Hz, 1H), 3.93 (s, 3H), 3.48 (dt, J = 11.5, 5.8 Hz, 1H), 2.80 (t, J = 6.0 Hz, 1H), 2.77–2.69 (m, 1H), 2.21–2.07 (m, 2H), 1.99–1.88 (m, 1H), 1.86–1.66 (m, 6H), 1.63–1.42 (m, 6H).

^{13}C NMR (126 MHz, DMSO-d_6): δ 166.1, 161.2, 153.7, 153.2, 134.3, 131.4, 130.9, 129.7, 127.9, 126.3, 124.4, 112.4, 110.2, 94.2, 79.9, 56.7, 55.6, 34.2, 33.3, 33.1, 30.2, 28.4, 28.4, 25.0, 24.9, 22.8, 22.4.

LC-MS (ESI): t_R = 5.58 min, area: 97%, m/z 444 $[M+H]$ +.

HRMS (ESI) m/z: $[M+H]$ + calcd. for $C_{27}H_{30}N_3O_3$ 444.2282, found 444.2266.

4.6.2.29. cis-5-(5-(3-Isopropyl-4-oxo-3,4,4a,5,8,8a-hexahydrophthalazin-1-yl)-2-methoxyphenyl)thiophene-2-carboxylic acid ***(18)***. To a solution of **17** (1.00 g, 2.65 mmol) and 5-borono-thiophene-2-carboxylic acid (0.830 g, 4.85 mmol) in DME (10 mL) was added aq. Na_2CO_3 (1 M, 6.6 mL, 6.63 mmol) and $PdCl_2$(dppf) (97.0 mg, 0.133 mmol). The reaction mixture was heated to 120 °C in the microwave for 3 h and then filtered over Celite using EtOAc (100 mL). The filtrate was washed with 1 M aq. HCl (2 × 150 mL), brine (10 mL), dried over $MgSO_4$, filtered and concentrated *in vacuo*. The residue was purified on a silica gel column eluting with EtOAc/*n*-heptane + 5% AcOH (gradient, 5–35%) to afford **18** as a white solid (610 mg, 49%).

^{1}H NMR (500 MHz, DMSO-d_6): δ 8.21 (d, J = 2.2 Hz, 1H), 7.89 (dd, J = 8.8, 2.2 Hz, 1H), 7.74 (d, J = 4.0 Hz, 1H), 7.70 (d, J = 4.0 Hz, 1H), 7.26 (d, J = 8.8 Hz, 1H), 5.74–5.60 (m, 2H), 4.89 (hept, J = 6.7 Hz, 1H), 3.99 (s, 3H), 3.58 (dt, J = 11.6, 5.8 Hz, 1H), 2.81 (t, J = 6.1 Hz, 1H), 2.79–2.72 (m, 1H), 2.23–2.10 (m, 2H), 1.86–1.77 (m, 1H), 1.25 (d, J = 6.5 Hz, 3H), 1.16 (d, J = 6.7 Hz, 3H).

^{13}C NMR (126 MHz, DMSO-d_6): δ 166.2, 163.4, 156.4, 153.4, 144.1, 134.6, 132.6, 127.8, 127.6, 126.4, 125.9, 125.3, 124.2, 121.6, 112.7, 56.2, 45.8, 34.0, 29.8, 22.6, 22.0, 20.6, 20.2.

LC-MS (ESI): t_R = 4.81 min, area: > 98%, m/z 425 $[M+H]^+$.

HRMS (ESI) m/z: $[M+H]^+$ calcd. for $C_{23}H_{25}N_2O_4S$ 425.1530, found 425.1541.

4.6.2.30. 5-(5-(cis-3-Isopropyl-4-oxo-3,4,4a,5,8,8a-hexahydrophthalazin-1-yl)-2-methoxyphenyl)thiophene-2-carboxamide ***(6a)***. To a solution of **18** (88.0 mg, 0.207 mmol) in DCM (2 mL) was added HOBt (73.0 mg, 0.540 mmol) and EDC.HCl (100 mg, 0.522 mmol). This mixture was stirred for 2 h at rt before NH_3 in MeOH (7 M, 0.5 mL, 3.50 mmol) was added. The reaction mixture was stirred for 22 h. EtOAc (2 × 10 mL) was added and the organic phase was washed with sat. aq. NH_4Cl (2 × 10 mL) and brine (5 mL), dried over $MgSO_4$, filtered and concentrated *in vacuo*. The residue was purified on a silica gel column eluting with EtOAc/*n*-heptane (gradient, 35–100%) to afford **6a** as a white solid (58 mg, 72%).

^{1}H NMR (500 MHz, $CDCl_3$): δ 8.13 (d, J = 2.2 Hz, 1H), 7.79 (dd, J = 8.7, 2.3 Hz, 1H), 7.55 (d, J = 4.0 Hz, 1H), 7.51 (d, J = 4.0 Hz, 1H), 7.04 (d, J = 8.8 Hz, 1H), 6.04 (s, 2H), 5.83–5.76 (m, 1H), 5.72–5.65 (m, 1H), 5.05 (hept, J = 6.6 Hz, 1H), 4.00 (s, 3H), 3.33 (dt, J = 11.6, 5.8 Hz, 1H), 3.07–2.98 (m, 1H), 2.76 (t, J = 6.0 Hz, 1H), 2.26–2.15 (m, 2H), 2.08–2.01 (m, 1H), 1.34 (d, J = 6.6 Hz, 3H), 1.22 (d, J = 6.7 Hz, 3H).

^{13}C NMR (126 MHz, $CDCl_3$): δ 166.5, 164.3, 157.0, 153.2, 144.6, 136.9, 129.1, 128.2, 127.3, 126.2, 126.1, 126.1, 124.0, 122.6, 111.7,

56.0, 46.9, 34.9, 31.2, 23.2, 22.5, 20.8, 20.4.

LC-MS (ESI): t_R = 4.47 min, area: 97%, *m/z* 424 $[M+H]^+$.

HRMS (ESI) *m/z*: $[M+H]^+$ calcd. for $C_{23}H_{26}N_3O_3S$ 424.1689, found 424.1683.

*4.6.2.31. N-Butyl-5-(5-(cis-3-isopropyl-4-oxo-3,4,4a,5,8,8a-hexahydrophthalazin-1-yl)-2-methoxyphenyl)thiophene-2-carboxamide (**6b**)*. This compound was prepared from **18** (88.0 mg, 0.207 mmol) and butan-1-amine (0.5 mL, 4.72 mmol) as described for **6a**. The title compound was obtained as a white solid (77 mg, 76%).

^{1}H NMR (500 MHz, $CDCl_3$): δ 8.11 (d, J = 2.3 Hz, 1H), 7.76 (dd, J = 8.7, 2.3 Hz, 1H), 7.51 (d, J = 4.0 Hz, 1H), 7.47 (d, J = 4.0 Hz, 1H), 7.02 (d, J = 8.7 Hz, 1H), 6.29–6.17 (m, 1H), 5.85–5.73 (m, 1H), 5.73–5.62 (m, 1H), 5.04 (hept, J = 6.8 Hz, 1H), 3.98 (s, 3H), 3.44 (q, J = 6.7 Hz, 2H), 3.33 (dt, J = 11.6, 5.8 Hz, 1H), 3.07–2.96 (m, 1H), 2.75 (t, J = 5.9 Hz, 1H), 2.27–2.13 (m, 2H), 2.08–1.99 (m, 1H), 1.60 (p, J = 7.4 Hz, 2H), 1.40 (h, J = 7.4 Hz, 2H), 1.33 (d, J = 6.6 Hz, 3H), 1.21 (d, J = 6.7 Hz, 3H), 0.95 (t, J = 7.4 Hz, 3H).

^{13}C NMR (126 MHz, $CDCl_3$): δ 166.5, 162.3, 156.9, 153.3, 143.1, 138.5, 128.1, 127.6, 127.0, 126.1, 126.1, 126.0, 124.0, 122.8, 111.7, 55.9, 46.8, 39.8, 34.8, 31.9, 31.1, 23.2, 22.4, 20.7, 20.3, 20.2, 13.9.

LC-MS (ESI): t_R = 5.30 min, area: > 98%, *m/z* 480 $[M+H]^+$.

HRMS (ESI) *m/z*: $[M+H]^+$ calcd. for $C_{27}H_{34}N_3O_3S$ 480.2315, found 480.2306.

*4.6.2.32. 5-(5-(cis-3-Isopropyl-4-oxo-3,4,4a,5,8,8a-hexahydrophthalazin-1-yl)-2-methoxyphenyl)-N-(2-methoxyethyl)thiophene-2-carboxamide (**6c**)*. This compound was prepared from **18** (212 mg, 0.50 mmol) and 2-methoxyethylamine (75 mg, 1.0 mmol) as described for **6a**. The title compound was obtained as a white solid (36 mg, 15%).

^{1}H NMR (250 MHz, $CDCl_3$): δ 8.12 (d, J = 2.05 Hz, 1H), 7.77 (dd, J = 2.21, 8.69 Hz, 1H), 7.53–7.43 (m, 2H), 7.03 (d, J = 8.69 Hz, 1H), 6.43 (t, J = 4.98 Hz, 1H), 5.86–5.60 (m, 2H), 5.15–4.95 (m, 1H), 3.99 (s, 3H), 3.72–3.50 (m, 4H), 3.40 (s, 3H), 3.37–3.26 (m, 1H), 3.10–2.92 (m, 1H), 2.76 (t, J = 5.77 Hz, 1H), 2.32–2.07 (m, 3H), 1.34 (d, J = 6.63 Hz, 3H), 1.27–1.12 (m, 3H)

^{13}C NMR (126 MHz, $CDCl_3$): δ 166.8, 162.6, 157.3, 153.5, 143.8, 138.4, 128.5, 128.2, 127.4, 126.3, 124.3, 123.0, 112.0, 77.7, 77.4, 71.6, 59.3, 56.2, 47.1, 40.0, 35.1, 31.5, 23.5, 22.7, 21.0, 20.6

LC-MS (ESI): t_R = 5.10 min, area: > 98%, *m/z* 482 $[M+H]^+$.

HRMS (ESI) *m/z*: $[M+H]^+$ calcd. for $C_{26}H_{32}N_3O_4$ 482.2108, found 482.2091.

*4.6.2.33. N-(Furan-2-ylmethyl)-5-(5-(cis-3-isopropyl-4-oxo-3,4,4a,5,8,8a-hexahydrophthalazin-1-yl)-2-methoxyphenyl)thiophene-2-carboxamide (**6d**)*. This compound was prepared from **18** (117 mg, 0.276 mmol) and furan-2-ylmethanamine (0.06 mL, 0.63 mmol) as described for **6a**. The title compound was obtained as a white solid (82 mg, 57%).

^{1}H NMR (500 MHz, $CDCl_3$): δ 8.12 (d, J = 2.3 Hz, 1H), 7.78 (dd, J = 8.7, 2.3 Hz, 1H), 7.52 (d, J = 4.0 Hz, 1H), 7.48 (d, J = 4.0 Hz, 1H), 7.42–7.33 (m, 1H), 7.03 (d, J = 8.7 Hz, 1H), 6.43 (t, J = 5.6 Hz, 1H), 6.35 (dd, J = 3.2, 1.8 Hz, 1H), 6.31 (d, J = 3.3 Hz, 1H), 5.84–5.75 (m, 1H), 5.75–5.61 (m, 1H), 5.05 (hept, J = 6.7 Hz, 1H), 4.64 (d, J = 5.4 Hz, 2H), 3.99 (s, 3H), 3.33 (dt, J = 11.6, 5.8 Hz, 1H), 3.09–2.94 (m, 1H), 2.76 (t, J = 6.0 Hz, 1H), 2.28–2.13 (m, 2H), 2.08–2.00 (m, 1H), 1.34 (d, J = 6.6 Hz, 3H), 1.21 (d, J = 6.7 Hz, 3H).

^{13}C NMR (126 MHz, $CDCl_3$): δ 166.5, 162.0, 157.0, 153.2, 151.2, 143.7, 137.6, 128.2, 128.2, 127.1, 126.1, 126.1, 126.0, 126.0, 124.0, 122.7, 111.7, 110.7, 107.9, 56.0, 46.9, 37.0, 34.9, 31.2, 23.2, 22.4, 20.7, 20.4.

LC-MS (ESI): t_R = 5.08 min, area: 97%, *m/z* 504 $[M+H]^+$.

HRMS (ESI) *m/z*: $[M+H]^+$ calcd. for $C_{28}H_{30}N_3O_4S$ 504.1952, found 504.1927.

*4.6.2.34. N-(2-Amino-2-oxoethyl)-5-(5-(cis-3-isopropyl-4-oxo-3,4,4a,5,8,8a-hexahydrophthalazin-1-yl)-2-methoxyphenyl)thiophene-2-carboxamide (**6e**)*. This compound was prepared from **18** (114 mg, 0.269 mmol) and glycinamide.HCl (74 mg, 0.67 mmol) as described for **6a**. The title compound was obtained as a white solid (88 mg, 63%).

^{1}H NMR (500 MHz, $CDCl_3$): δ 8.11 (d, J = 2.2 Hz, 1H), 7.77 (dd, J = 8.7, 2.3 Hz, 1H), 7.62 (d, J = 4.0 Hz, 1H), 7.49 (d, J = 4.0 Hz, 1H), 7.24 (t, J = 5.3 Hz, 2H), 7.02 (d, J = 8.8 Hz, 1H), 6.61 (s, 1H), 5.85–5.75 (m, 2H), 5.71–5.65 (m, 1H), 5.04 (hept, J = 6.7 Hz, 1H), 4.18 (d, J = 5.1 Hz, 2H), 3.97 (s, 3H), 3.32 (dt, J = 11.6, 5.8 Hz, 1H), 3.05–2.97 (m, 1H), 2.75 (t, J = 6.0 Hz, 1H), 2.25–2.14 (m, 2H), 2.07–1.99 (m, 1H), 1.33 (d, J = 6.6 Hz, 3H), 1.21 (d, J = 6.7 Hz, 3H).

^{13}C NMR (126 MHz, $CDCl_3$): δ 171.5, 166.5, 162.9, 157.0, 153.2, 144.2, 137.0, 128.7, 128.2, 127.2, 126.1, 126.0, 124.0, 122.6, 111.7, 56.0, 46.9, 43.4, 34.9, 31.2, 23.2, 22.5, 20.8, 20.4.

LC-MS (ESI): t_R = 4.19 min, area: 95%, *m/z* 481 $[M+H]^+$.

HRMS (ESI) *m/z*: $[M+H]^+$ calcd. for $C_{25}H_{29}N_4O_4$ 481.1904, found 481.1924.

*4.6.2.35. cis-1-(5-(3-Isopropyl-4-oxo-3,4,4a,5,8,8a-hexahydrophthalazin-1-yl)-2-methoxyphenyl)azetidine-3-carbonitrile (**19**)*. To a solution of **17** (2.60 g, 6.89 mmol) in dry toluene (15 mL) was added Xantphos (0.798 g, 1.38 mmol), Pd(II)$(OAc)_2$ (0.155 g, 0.689 mmol), Cs_2CO_3 (4.49 g, 13.8 mmol) and azetidine-3-carbonitrile.HCl (0.577 g, 6.89 mmol). The mixture was stirred at 100 °C for 68 h. The reaction mixture was filtered over celite with EtOAc (2 × 50 mL). The filtrate was washed with sat. aq. NH_4Cl (2 × 25 mL) and brine (20 mL). The organic phase was dried over $MgSO_4$, filtered and concentrated *in vacuo*. The residue was purified on a silica gel column eluting with EtOAc/*n*-heptane (gradient, 5–40%) to afford **19** as a white solid (1.21 g, 46%).

^{1}H NMR (500 MHz, $CDCl_3$): δ 7.23 (dd, J = 8.4, 2.1 Hz, 1H), 7.04 (d, J = 2.1 Hz, 1H), 6.81 (d, J = 8.4 Hz, 1H), 5.83–5.62 (m, 2H), 5.04 (hept, J = 6.6 Hz, 1H), 4.29 (td, J = 7.9, 4.2 Hz, 2H), 4.12 (td, J = 7.2, 1.7 Hz, 2H), 3.85 (s, 3H), 3.61–3.51 (m, 1H), 3.28 (dt, J = 11.5, 5.8 Hz, 1H), 3.05–2.96 (m, 1H), 2.72 (t, J = 5.9 Hz, 1H), 2.25–2.10 (m, 2H), 2.06–1.96 (m, 1H), 1.32 (d, J = 6.6 Hz, 3H), 1.20 (d, J = 6.7 Hz, 3H).

^{13}C NMR (126 MHz, $CDCl_3$): δ 166.5, 153.7, 151.0, 139.8, 128.2, 126.1, 124.1, 120.0, 119.1, 110.6, 110.2, 56.7, 56.6, 55.7, 46.8, 34.8, 31.1, 23.3, 22.5, 20.7, 20.3, 19.1.

LC-MS (ESI): t_R = 4.45 min, area: > 98%, *m/z* 379 $[M+H]^+$.

HRMS (ESI) *m/z*: $[M+H]^+$ calcd. for $C_{22}H_{27}N_4O_2$ 379.2129, found 379.2128.

*4.6.2.36. cis-1-(5-(3-Isopropyl-4-oxo-3,4,4a,5,8,8a-hexahydrophthalazin-1-yl)-2-methoxyphenyl)azetidine-3-carboxylic acid (**20**)*. A solution of **19** (1.05 g, 2.77 mmol) in EtOH (2.7 mL) and aq. NaOH (1 M, 2.7 mL, 2.7 mmol) was stirred at 75 °C for 24 h. EtOAc (2 × 10 mL) was added and the organic phase was washed with sat. aq. NH_4Cl (2 × 10 mL) and brine (5 mL). The combined organic phases were dried over $MgSO_4$, filtered and concentrated *in vacuo* to afford **20** as a white solid (0.55 g, 47%).

^{1}H NMR (500 MHz, DMSO-d_6): δ 7.18 (d, J = 8.3 Hz, 1H), 6.95–6.88 (m, 1H), 6.86 (d, J = 8.5 Hz, 1H), 5.71–5.64 (m, 1H), 5.64–5.57 (m, 1H), 4.85 (hept, J = 6.8 Hz, 1H), 4.06–3.94 (m, 2H), 3.92–3.85 (m, 2H), 3.73 (s, 3H), 3.37 (dt, J = 11.6, 5.7 Hz, 1H), 3.31–3.25 (m, 1H), 2.80–2.65 (m, 2H), 2.23–2.10 (m, 1H), 2.10–2.01 (m, 1H), 1.84–1.72 (m, 1H), 1.21 (d, J = 6.7 Hz, 3H), 1.11 (d, J = 6.7 Hz, 3H).

^{13}C NMR (126 MHz, DMSO-d_6): δ 166.0, 154.0, 150.4, 141.4, 127.5, 126.0, 124.2, 117.4, 111.0, 109.2, 56.5, 55.6, 45.7, 45.4, 34.0, 30.0, 22.9, 22.1, 20.5, 20.2.

LC-MS (ESI): t_R = 4.55 min, area: 96%, *m/z* 398 $[M+H]^+$.

HRMS (ESI) *m/z*: $[M+H]^+$ calcd. for $C_{22}H_{28}N_3O_4$ 398.2074, found 398.2060.

*4.6.2.37. 1-(5-(cis-3-Isopropyl-4-oxo-3,4,4a,5,8,8a-hexahydrophthalazin-1-yl)-2-methoxyphenyl)azetidine-3-carboxamide (**7a**)*. This compound

was prepared from **20** (110 mg, 0.277 mmol) and NH_3 in MeOH (7 M, 1.6 mL, 11 mmol) as described for **6a**. The title compound was obtained as a white solid (63 mg, 56%).

^{1}H NMR (500 MHz, DMSO-d_6): δ 7.45 (s, 1H), 7.21 (dd, J = 8.5, 2.1 Hz, 1H), 7.00 (s, 1H), 6.95–6.86 (m, 2H), 5.77–5.54 (m, 2H), 4.86 (hept, J = 6.7 Hz, 1H), 4.00 (q, J = 7.4 Hz, 2H), 3.84 (q, J = 6.9 Hz, 2H), 3.76 (s, 3H), 3.42–3.37 (m, 2H), 2.81–2.67 (m, 2H), 2.22–2.02 (m, 2H), 1.85–1.74 (m, 1H), 1.23 (d, J = 6.4 Hz, 3H), 1.13 (d, J = 6.8 Hz, 3H).

^{13}C NMR (126 MHz, DMSO-d_6): δ 173.7, 166.0, 154.0, 150.4, 141.2, 127.5, 126.0, 124.2, 117.6, 111.0, 109.3, 55.9, 55.8, 55.6, 45.7, 34.3, 34.0, 30.0, 22.8, 22.0, 20.5, 20.2.

LC-MS (ESI): t_R = 4.13 min, area: > 98%, m/z 397 $[M+H]^+$.

HRMS (ESI) m/z: $[M+H]^+$ calcd. for $C_{22}H_{29}N_4O_3$ 397.2234, found 397.2216.

*4.6.2.38. N-Butyl-1-(5-(cis-3-isopropyl-4-oxo-3,4,4a,5,8,8a-hexahydrophthalazin-1-yl)-2-methoxyphenyl)azetidine-3-carboxamide (**7b**)*. This compound was prepared from **20** (94.0 mg, 0.236 mmol) and butan-1-amine (0.5 mL, 5.20 mmol) as described for **6a**. The title compound was obtained as a white solid (34 mg, 31%).

^{1}H NMR (500 MHz, DMSO-d_6): δ 7.94 (t, J = 5.6 Hz, 1H), 7.21 (dd, J = 8.4, 2.1 Hz, 1H), 6.99–6.84 (m, 2H), 5.74–5.57 (m, 2H), 4.86 (hept, J = 5.3 Hz, 1H), 4.01 (q, J = 7.4 Hz, 2H), 3.83 (q, J = 6.7 Hz, 2H), 3.76 (s, 3H), 3.46–3.38 (m, 2H), 3.05 (q, J = 6.6 Hz, 2H), 2.82–2.67 (m, 2H), 2.21–2.02 (m, 2H), 1.86–1.74 (m, 1H), 1.37 (p, J = 7.0 Hz, 2H), 1.32–1.18 (m, 5H), 1.12 (d, J = 6.7 Hz, 3H), 0.86 (t, J = 7.3 Hz, 3H).

^{13}C NMR (126 MHz, DMSO-d_6): δ 171.3, 166.0, 154.1, 150.4, 141.2, 127.5, 126.0, 124.2, 117.6, 111.1, 109.4, 55.9, 55.8, 55.6, 45.7, 38.3, 34.4, 34.0, 31.2, 30.0, 22.8, 22.0, 20.5, 20.2, 19.6, 13.8.

LC-MS (ESI): t_R = 5.02 min, area: > 98%, m/z 453 $[M+H]^+$.

HRMS (ESI) m/z: $[M+H]^+$ calcd. for $C_{26}H_{37}N_4O_3$ 453.2860, found 453.2846.

*4.6.2.39. N-(Furan-2-ylmethyl)-1-(5-(cis-3-isopropyl-4-oxo-3,4,4a,5,8,8a-hexahydrophthalazin-1-yl)-2-methoxyphenyl)azetidine-3-carboxamide (**7c**)*. This compound was prepared from **20** (110 mg, 0.277 mmol) and furan-2-ylmethanamine (0.06 mL, 0.679 mmol) as described for **6a**. The title compound was obtained as a white solid (93 mg, 64%).

^{1}H NMR (500 MHz, DMSO-d_6): δ 8.47 (t, J = 5.6 Hz, 1H), 7.58 (d, J = 1.4 Hz, 1H), 7.22 (dd, J = 8.5, 2.2 Hz, 1H), 6.91 (d, J = 2.1 Hz, 1H), 6.89 (d, J = 8.5 Hz, 1H), 6.39 (dd, J = 3.2, 1.9 Hz, 1H), 6.24 (d, J = 3.1 Hz, 1H), 5.72–5.66 (m, 1H), 5.66–5.58 (m, 1H), 4.86 (hept, J = 6.7 Hz, 1H), 4.28 (d, J = 5.5 Hz, 2H), 4.02 (q, J = 7.3 Hz, 2H), 3.86 (q, J = 6.7 Hz, 2H), 3.76 (s, 3H), 3.47–3.38 (m, 2H), 2.79–2.69 (m, 2H), 2.21–2.02 (m, 2H), 1.85–1.74 (m, 1H), 1.23 (d, J = 6.6 Hz, 3H), 1.13 (d, J = 6.7 Hz, 3H).

^{13}C NMR (126 MHz, DMSO-d_6): δ 171.5, 166.0, 154.0, 152.2, 150.4, 142.2, 141.1, 127.5, 126.0, 124.2, 117.6, 111.1, 110.5, 109.4, 107.0, 55.8, 55.7, 55.6, 45.7, 35.6, 34.3, 34.0, 30.0, 22.8, 22.0, 20.5, 20.2.

LC-MS (ESI): t_R = 4.85 min, area: 97%, m/z 477 $[M+H]^+$.

HRMS (ESI) m/z: $[M+H]^+$ calcd. for $C_{27}H_{33}N_4O_4$ 477.2496, found 477.2481.

*4.6.2.40. N-(2-Amino-2-oxoethyl)-1-(5-(cis-3-isopropyl-4-oxo-3,4,4a,5,8,8a-hexahydrophthalazin-1-yl)-2-methoxyphenyl)azetidine-3-carboxamide (**7d**)*. This compound was prepared from **20** (110 mg, 0.277 mmol) and glycinamide.HCl (76 mg, 1.0 mmol) as described for **6a**. The title compound was obtained as a white solid (90 mg, 70%).

^{1}H NMR (500 MHz, DMSO-d_6): δ 8.19 (t, J = 5.9 Hz, 1H), 7.36 (s, 1H), 7.21 (dd, J = 8.5, 2.1 Hz, 1H), 7.05 (s, 1H), 6.91 (d, J = 2.1 Hz, 1H), 6.89 (d, J = 8.5 Hz, 1H), 5.75–5.65 (m, 1H), 5.65–5.56 (m, 1H), 4.86 (hept, J = 6.7 Hz, 1H), 4.02 (q, J = 7.3 Hz, 2H), 3.86 (q, J = 6.7 Hz, 2H), 3.76 (s, 3H), 3.65 (d, J = 5.8 Hz, 2H), 3.48 (p, J = 7.4 Hz, 1H), 3.41–3.36 (m, 4H), 2.79–2.68 (m, 2H), 2.22–2.02 (m, 2H), 1.86–1.73 (m, 1H), 1.23 (d, J = 6.6 Hz, 3H), 1.13 (d, J = 6.7 Hz, 3H).

^{13}C NMR (126 MHz, DMSO-d_6): δ 172.0, 171.0, 166.0, 154.1, 150.4, 141.2, 127.5, 126.0, 124.2, 117.6, 111.0, 109.3, 55.9, 55.8, 55.6, 45.7, 42.0, 34.4, 34.0, 30.0, 22.9, 22.1, 20.5, 20.2.

LC-MS (ESI): t_R = 3.90 min, area: > 98%, m/z 454 $[M+H]^+$.

HRMS (ESI) m/z: $[M+H]^+$ calcd. for $C_{24}H_{32}N_5O_4$ 454.2449, found 454.2442.

Acknowledgements

We thank N. Koning, C.G.W. van Melis and F.G.J. Custers for synthetic and analytical support. We thank A.J. Kooistra for the help with docking. We also thank staff of Diamond Light Source beam lines I04 and I04-1 for their help in X-ray data collection. Funding: This work was supported by TI Pharma, Netherlands [grant number T4-302] and the European Commission 7th Framework Programme FP7-HEALTH-2013-INNOVATION-1 under project reference 602666 “Parasite-specific cyclic nucleotide phosphodiesterase inhibitors to target Neglected Parasitic Diseases” (PDE4NPD).

Declaration of Competing Interest

None.

Author contributions

E.d.H., E.E., M.P.K.J., T.v.d.B., J.V., G.J.S. and I.J.P.d.E. were involved in compound design, synthesis and analysis. A.K.S. and D.G.B. were involved in protein production, crystallization, data collection and refinement for structural studies. E.d.H., A.K.S. and D.G.B. were involved in crystal structure analysis. T.v.d.M., M.v.d.W., P.S. and M.S. were involved in the biochemical assays. G.C. and L.M. were involved in the phenotypic cellular assays and T.D.K. performed the target validation experiments, supervised by H.P.d.K. E.E., M.W., M.S., L.M., G.J.S., I.J.P.d.E., D.G.B. and R.L. supervised the experiments and conceived the project. E.d.H., A.K.S., G.J.S., I.J.P.d.E., H.P.d.K., D.G.B. and R.L. integrated all data and wrote the manuscript.

Appendix A. Supplementary data

Supplementary data to this article can be found online at https://doi.org/10.1016/j.bmc.2019.06.027.

References

1. Büscher P, Cecchi G, Jamonneau V, Priotto G. Human African trypanosomiasis. *Lancet.* 2017;390:2397–2409.
2. Brun R, Blum J, Chappuis F, Burri C. Human african trypanosomiasis. *Lancet.* 2010;375:148–159.
3. Feasey N, Wansbrough-Jones M, Mabey DC, Solomon AW. Neglected tropical diseases. *Br Med Bull.* 2010;93:179–200.
4. Babokhov P, Sanyaolu AO, Oyibo WA, Fagbenro-Beyioku AF, Iriemenam NC. A current analysis of chemotherapy strategies for the treatment of human African trypanosomiasis. *Pathog Global Health.* 2013;107:242–252.
5. Fairlamb AH. Chemotherapy of human African trypanosomiasis: current and future prospects. *Trends Parasitol.* 2003;19:488–494.
6. Delespaux V, de Koning HP. Drugs and drug resistance in African trypanosomiasis. *Drug Resist Updates.* 2007;10:30–50.
7. Eperon G, Balasegaram M, Potet J, Mowbray C, Valverde O, Chappuis F. Treatment options for second-stage gambiense human African trypanosomiasis. *Expert Rev Anti Infect Ther.* 2014;12:1407–1417.
8. Kennedy PGE. Human African trypanosomiasis of the CNS: current issues and challenges. *J Clin Invest.* 2004;113:496–504.
9. de Koning HP. Drug resistance in protozoan parasites. *Emerging Top Life Sci.* 2017;1:627.
10. Munday JC, Settimo L, de Koning HP. Transport proteins determine drug sensitivity and resistance in a protozoan parasite, Trypanosoma brucei. *Front Pharmacol.* 2015;6.
11. Calverley PMA, Rabe KF, Goehring U-M, Kristiansen S, Fabbri LM, Martinez FJ. Roflumilast in symptomatic chronic obstructive pulmonary disease: two randomised

clinical trials. *Lancet.* 2009;374:685–694.
12. Hatzelmann A, Schudt C. Anti-Inflammatory and Immunomodulatory Potential of the Novel PDE4 Inhibitor Roflumilast in Vitro. *J Pharmacol Exp Ther.* 2001;297:267–279.
13. Packer M, Carver JR, Rodeheffer RJ, et al. Effect of oral milrinone on mortality in severe chronic heart failure. *N Engl J Med.* 1991;325:1468–1475.
14. Boolell M, Allen MJ, Ballard SA, et al. Sildenafil: an orally active type 5 cyclic GMP-specific phosphodiesterase inhibitor for the treatment of penile erectile dysfunction. *Int J Impot Res.* 1996;8:47–52.
15. Oberholzer M, Marti G, Baresic M, Kunz S, Hemphill A, Seebeck T. The Trypanosoma brucei cAMP phosphodiesterases TbrPDEB1 and TbrPDEB2: flagellar enzymes that are essential for parasite virulence. *FASEB J.* 2007;21:720–731.
16. Kunz S, Beavo JA, D'Angelo MA, et al. Cyclic nucleotide specific phosphodiesterases of the kinetoplastida: a unified nomenclature. *Mol Biochem Parasitol.* 2006;145:133–135.
17. Amata E, Bland ND, Campbell RK, Pollastri MP. Evaluation of pyrrolidine and pyrazolone derivatives as inhibitors of trypanosomal phosphodiesterase B1 (TbrPDEB1). *Tetrahedron Lett.* 2015;56:2832–2835.
18. Amata E, Bland ND, Hoyt CT, Settimo L, Campbell RK, Pollastri MP. Repurposing human PDE4 inhibitors for neglected tropical diseases: design, synthesis and evaluation of cilomilast analogues as Trypanosoma brucei PDEB1 inhibitors. *Bioorg Med Chem Lett.* 2014;24:4084–4089.
19. Jansen C, Wang H, Kooistra AJ, et al. Discovery of NovelTrypanosoma bruceiPhosphodiesterase B1 inhibitors by virtual screening against the unliganded tbrpdeb1 crystal structure. *J Med Chem.* 2013;56:2087–2096.
20. Ochiana SO, Bland ND, Settimo L, Campbell RK, Pollastri MP. Repurposing human PDE4 inhibitors for neglected tropical diseases. Evaluation of analogs of the human PDE4 inhibitor GSK-256066 as inhibitors of PDEB1 of Trypanosoma brucei. *Chem Biol Drug Des.* 2014.
21. Wang C, Ashton TD, Gustafson A, et al. Synthesis and evaluation of human phosphodiesterases (PDE) 5 inhibitor analogs as trypanosomal PDE inhibitors. Part 1. Sildenafil analogs. *Bioorg Med Chem Lett.* 2012;22:2579–2581.
22. Woodring JL, Bland ND, Ochiana SO, Campbell RK, Pollastri MP. Synthesis and assessment of catechol diether compounds as inhibitors of trypanosomal phosphodiesterase B1 (TbrPDEB1). *Bioorg Med Chem Lett.* 2013;23:5971–5974.
23. Blaazer AR, Orrling KM, Shanmugham A, et al. Fragment-based screening in tandem with phenotypic screening provides novel antiparasitic hits. *J Biomol Screen.* 2015;20:131–140.
24. Orrling KM, Jansen C, Vu XL, et al. Catechol pyrazolinones as trypanocidals: fragment-based design, synthesis, and pharmacological evaluation of nanomolar inhibitors of trypanosomal phosphodiesterase B1. *J Med Chem.* 2012;55:8745–8756.
25. de Koning HP, Gould MK, Sterk GJ, et al. Pharmacological validation of Trypanosoma brucei phosphodiesterases as novel drug targets. *J Infect Dis.* 2012;206:229–237.
26. Van der Mey M, Hatzelmann A, Van der Laan IJ, Sterk GJ, Thibaut U, Timmerman H. Novel selective PDE4 inhibitors. 1. synthesis, structure-activity relationships, and molecular modeling of 4-(3, 4-dimethoxyphenyl)-2 H-phthalazin-1-ones and analogues. *J Med Chem.* 2001;44:2511–2522.
27. Van der Mey M, Hatzelmann A, Van Klink GPM, et al. Novel selective PDE4 inhibitors. 2. synthesis and structure-activity relationships of 4-aryl-substituted cis-tetra- and cis-hexahydrophthalazinones. *J Med Chem.* 2001;44:2523–2535.
28. Veerman J, van den Bergh T, Orrling KM, et al. Synthesis and evaluation of analogs of the phenylpyridazinone NPD-001 as potent trypanosomal TbrPDEB1 phosphodiesterase inhibitors and in vitro trypanocidals. *Biorg Med Chem.* 2016;24:1573–1581.
29. Souness JE, Rao S. Proposal for pharmacologically distinct conformers of PDE4 cyclic AMP phosphodiesterases. *Cell Signal.* 1997;9:227–236.
30. Boswell-Smith V, Spina D, Page CP. Phosphodiesterase inhibitors. *Br J Pharmacol.* 2006;147:S252–S257.
31. Seldon PM, Barnes PJ, Meja K, Giembycz MA. Suppression of lipopolysaccharide-induced tumor necrosis factor-alpha generation from human peripheral blood monocytes by inhibitors of phosphodiesterase 4: interaction with stimulants of adenylyl cyclase. *Mol Pharmacol.* 1995;48:747–757.
32. Blaazer AR, Singh AK, de Heuvel E, et al. Targeting a subpocket in Trypanosoma brucei phosphodiesterase B1 (TbrPDEB1) enables the structure-based discovery of selective inhibitors with trypanocidal activity. *J Med Chem.* 2018.
33. Seebeck T, Sterk GJ, Ke H. Phosphodiesterase inhibitors as a new generation of antiprotozoan drugs: exploiting the benefit of enzymes that are highly conserved between host and parasite. *Future Med Chem.* 2011;3:1289–1306.
34. Phoujdar MS, Kathiravan MK, Bariwal JB, Shah AK, Jain KS. Microwave-based synthesis of novel thienopyrimidine bioisosteres of gefitinib. *Tetrahedron Lett.* 2008;49:1269–1273.
35. Winter G, Lobley CMC, Prince SM. Decision making in xia2. *Acta Crystallogr Sect D.* 2013;69:1260–1273.
36. Kabsch W. Integration, scaling, space-group assignment and post-refinement. *Acta Crystallogr Sect D.* 2010;66:133–144.
37. Evans PR, Murshudov GN. How good are my data and what is the resolution? *Acta Crystallogr Sect D.* 2013;69:1204–1214.
38. Battye TGG, Kontogiannis L, Johnson O, Powell HR, Leslie AGW. iMOSFLM: a new graphical interface for diffraction-image processing with MOSFLM. *Acta Crystallogr Sect D.* 2011;67:271–281.
39. Winn MD, Ballard CC, Cowtan KD, et al. Overview of the CCP4 suite and current developments. *Acta Crystallogr Sect D.* 2011;67:235–242.
40. McCoy AJ, Grosse-Kunstleve RW, Adams PD, Winn MD, Storoni LC, Read RJ. Phaser crystallographic software. *J Appl Crystallogr.* 2007;40:658–674.
41. Emsley P, Lohkamp B, Scott WG, Cowtan K. Features and development of Coot. *Acta Crystallogr Sect D.* 2010;66:486–501.
42. Murshudov GN, Skubak P, Lebedev AA, et al. REFMAC5 for the refinement of macromolecular crystal structures. *Acta Crystallogr Sect D.* 2011;67:355–367.
43. The PyMOL Molecular Graphics System, Version 1.7, Schrödinger, LLC.